Master thesis

Modelling Energy Efficient Data Transmissions

performed under the direction of

Univ.Prof. Dipl.-Ing. Dr.techn. Markus Rupp

Dipl.-Ing. Dr.techn. Philipp Svoboda

submitted at the

Technical University of Wien

Faculty of Electrical Engineering and Information Technology

Institute of Telecommunications

by

Gonzalo Iglesias Cayuela

Juli, 2014

I hereby declare that this thesis is my original work and it has been written by me in its entirety.

I have acknowledged all the sources of information which have been used in the thesis.

Gonzalo Iglesias Cayuela

Vienna, July 2014

Abstract

In 2014 the mobile traffic is growing very rapidly, approximately each year it's the double of the previous year and this growth is projected to continue unabated. Thus, the mobile industry needs to prepare for the challenge of meeting an increase on mobile data demand, because with the introduction of smartphones, tablets and USB modems, mobile devices have been evolved into a versatile communication companion. But, while mobile traffic has been growing, the battery capacity increases slightly over the years, in other words, it is not growing fast enough to cope with the needs required by the devices.

In this project we are interested in metering the energy consumption of the User Equipment in a cellular mobile radio network. The goal of the master Thesis is to measure and evaluate the power per bit and setup for different scenarios for UMTS and LTE and find a model for the power per bit consumption. To that end, has been implemented a Java program to measure the relationship between the data rate and the energy consumed by a hardware Power Meter, and once taken multiple measurements with a USB modem, finally by Matlab, the distribution model for the energy consumed has been found.

Acknoledgements.

I want to thank in first place to my supervisor Philipp Svoboda for his help, patience and guidance that he granted me since my first days in Vienna.

Secondly, I want to thank to my family, especially my parents and brother for their care and for trusting always in me and to my godparents for their support.

And finally I want to thank to my friends, for all the good moments

Contents

Chapter 1

Introduction

1.1. The origin (0G).

The origin of the mobile phone dates back to the beginning of World War II. During those years, Motorola has created a team called Handie Talkie H12-16, allowing contact with the troops via radio waves whose frequency band at that time did not exceed 60 MHz.

Since the early 70's in the U.S., Martin Cooper, also from Motorola, was the pioneer in introducing the first mobile phone, known as Dyna-Trac in 1973, which is why it is regarded as "the father of the cell phone ". But it was not until 1979 when the first commercial systems in Tokyo, Japan, appeared by NTT (Nippon Telegraph and Telephone Corporation). Just in 1982 the U.S. Federal Communications Commission approved the launch of the first commercial mobile system for the company Ameritech [1].

To separate one stage from the other, the cell phone has been characterized by having different generations. Below is a summary of each of them.

1.2 First generation (1G).

The First Generation of mobile communications is based on FDMA (Frequency Division Multiple Access) and is characterized by analog and strictly for voice. The predominant technology of this generation is AMPS (Advanced Mobile Phone System) used mainly in the United States [2].

1.3. Second generation (2G).

2G is not a standard or a protocol in itself, but rather a way to mark the change of analog to digital mobile communication, with the addition of TDMA (Time Division Multiple Access). 2G arrived around 1990 and the development led to the need to handle increased call handling substantially in the same frequency spectrums. The predominant technologies are: GSM (Global System for Mobile Communications), IS-136 (also known as TIA/EIA136 or ANSI-136), CDMA (Code Division Multiple Access) and PDC (Personal Digital Communications), the latter used in Japan.

2G, to meet a higher requirement on data transmission rates, evolved from three TDMA updates: High Speed Circuit Switched Data (HSCSD), General Packet Radio Service (GPRS) and Enhanced Data Rate for GSM Evolution (EDGE), the latter commercially categorized as 2.75G and 2.5 respectively and that are characterized by incorporating packet-switching nodes (Packet-Switched) to existing circuit-switched node (Circuit-Switched) [3].

1.4. Third generation (3G).

The 3G mobile communication systems are characterized by the convergence of voice and data access; in other words, it is suitable for multimedia and high rates of data transmission applications.

Systems of this standard are essentially a linear improvement of 2G systems and, as its intermediate evolution, it is based on a parallel backbone infrastructure, consisting on the one hand in circuit-switching nodes and secondly in packet-switching nodes (circuit-switched and packet-switched domains).

The International Telecommunication Union (ITU) defined the demands for 3G networks under the IMT-2000 standard. This system was developed primarily under the UMTS (Universal Mobile Telecommunications System) using WCDMA.

More information can be found in this thesis in chapter 3.2.

1.5. Fourth generation (4G).

4G stands for fourth generation mobile communication systems and is based entirely on IP, being considered a system of systems and a network of networks. 4G is used broadly to define various types of mobile broadband access, not only cellular telephone systems, to provide access speeds between 100 Mbps and 1Gbps both Indoor and outdoor, with high quality of service (QoS) and optimum security, allowing the supply of services of any kind in anytime, anywhere, with minimal cost.

More information is included in this thesis in chapter 3.2.

Chapter 2.

Project scope.

2.1. Background.

Global mobile data traffic will grow by a factor of 11 in the next four years, reaching 190 exabytes per year in 2018, representing a ratio of increase of 57 percent in that period (2014-2018).

This significant increase is due in part to the exponential increase in the number of mobile internet connections (such as personal devices and machine-to-machine connections), which exceed 10,000 million and is 1.4 times higher than the global population expected in 2018.

Between 2014 and 2018, it is expected that the growth of global mobile data traffic will surpass almost three times the growth of global fixed data traffic, with several major trends responsible for this growth [4]:

- More mobile users: in 2018 there will be 4,900 million mobile users (4,100 million recorded in 2013).

- More mobile connections: in 2018 there will be over 10,000 million devices / phones, including 8,000 million personal connections and 2,000 million mobile connections machine to machine (M2M). 7,000 million M2M devices and connections were recorded in 2013.

- Faster mobile connections: the overall average speed of mobile network connections will be almost doubled between 2012 (1.4 Mbps) and 2018 (2.5 Mbps).

- More mobile video: in 2018 the Global mobile video traffic will account for 69 percent of all global mobile data traffic (53 percent in 2013).

- Evolution towards smart devices: 54 percent of global mobile connections will be 'smart' in 2018, from 21 percent recorded in 2013. The devices and connections have intelligent advanced computing capabilities, multimedia and 3G connectivity at least. Smartphones, laptops and tablets will generate about 94 percent of global mobile data traffic in 2018. The M2M traffic will account for 5 percent of all global mobile data traffic in 2018, while the remaining 1 percent corresponds to basic terminals and 0.1 percent to other portable devices.

- More mobile Cloud traffic: globally, cloud applications will account for 90 percent of total mobile data traffic by 2018, compared to 82 percent at the end of 2013.

- Impact of faster mobile connections: it is expected that the average speed of mobile connections will be doubled between 2014 and 2018. This speed is a key to support the expected increase in global mobile data traffic.

- 4G technology adoption and growth of traffic: in 2018 4G connections will support 15 percent of all connections, from 2.9 percent in 2013.
  A large number of service providers worldwide are deploying 4G technologies to meet the increased demand for wireless services and content by consumers and businesses. In many emerging market, operators are building new 4G mobile network solutions. In advanced markets, service providers are completing or replacing legacy networks (2G/3G) with 4G technologies.
  In 2018 4G connections will support 51 percent (8 Exabytes monthly) of all mobile data traffic, from 30 percent (448 petabytes per month) in 2013.
  The 4G traffic will grow 18-fold between 2013 and 2018 (annual increase of 78 percent).

- The video is still in the lead: about of mobile traffic in applications, mobile video traffic will be multiplied by 12 between 2014 and 2018, accumulating the highest growth rate in the category of mobile applications.
  In 2018 mobile video will account for 69 percent of all global mobile traffic, from 53 percent in 2013 [7].

2.2. Motivations.

The gap between available and required energy in battery supplied wireless user equipment (UE) is increasing year by year.

Although new materials are being investigated such as silicon, graphene, sodium or even sugar, the vast majority of smartphones use rechargeable electrochemical batteries, usually lithium-ion (Li-ion). The problem with these batteries is their short duration when connections to data networks are maintained. As a result of not being able to increase the capacity of the batteries, it is necessary that the devices themselves reduce power consumption levels to improve the use experience of users [5].

The main motivation of this project has been to find a way to reduce that level of power consumption, finding a statistical distribution model that allows knowing in advance the amount of energy required to make the mobile use of UMTS and LTE, since the transfer of data via mobile networks is what consumes more power on a Smartphone.

To perform this task, a series of objectives that are detailed in the following section, has been conducted.

2.3. Objectives.

The main objective has been to find a probability distribution model for data in 3G and LTE regarding the energy consumed.

This principle objective of the master thesis has been divided in different goals:

- Measurement setup: preparing the hardware and software that will be used later to take the measurements.
- Conduct measurements: taking measures for videostreaming, emails sending and web traffic over 3G and LTE.
- Derive model for energy consumption per bit: based on the measures that have been taken throughout the project.

2.4. Project structure.

Briefly it will be commented in which will consist each chapter of this master thesis.

First, in the chapter 3 “Mobile technologies”, it will be explained the theoretical fundamentals of the two mobile technologies in which measurements have been taken: UMTS and LTE.

Next, in the chapter 4 “Measurement setup”, it will be talked about the hardware that it has been used and the software that was developed for doing the measurements.

After that, in the chapter 5 “Measurements”, it will be commented the different scenarios for doing the measurements and the results that have been obtained from these measurements.

Later, in the chapter 6 “Distribution model”, it will be described the distribution model that was chosen based on the results.

Finally, in the chapter 7 “Conclusions and outlook”, it will be presented the conclusions that have been extracted from this master thesis and a possible future work.

Chapter 3.

Mobile Technologies.

3.1. UMTS.

3.1.1. Introduction.

Universal Mobile Telecommunications System (UMTS) is compatible with mobile multimedia applications with high data transmission rates. Figure 1 depicts a simplified UMTS architecture, which consists of the *Core Network* and the *UMTS Terrestrial Radio Access Network* (UTRAN). The core network is responsible for switching or routing calls and data connections to the external networks, and the UTRAN deals with all radio-related features [8]. The UTRAN consists of *Radio Network Controllers* (RNCs) and *Node Bs* (i.e., base stations) that are connected by an *Asynchronous Transfer Mode* (ATM) network. A *Mobile Station* (MS) communicates with Node Bs through the radio interface based on the WCDMA (Wideband CDMA) technology [9].

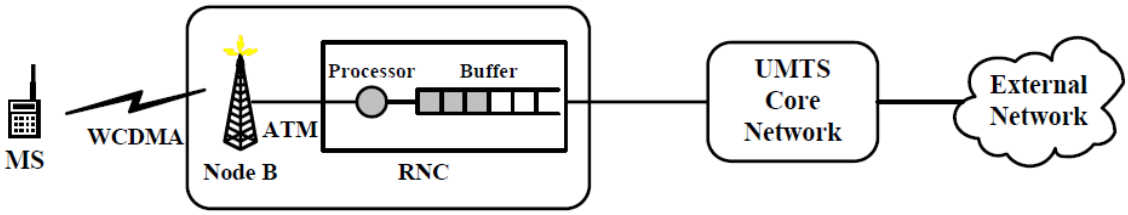

MS: Mobile Station RNC: Radio Network Controller
Node B: Base Station UTRAN: UMTS Terrestrial Radio Access Network

Figure 3.1: A simplified UMTS network architecture.

3.1.2. Discontinuous reception.

In UMTS, MS power consumption is an important problem for wireless data transmission. The data bandwidth is significantly limited by the battery capacity. Therefore, power saving mechanisms are typically exercised to reduce power consumption. Most existing wireless mobile networks (including UMTS) employ *Discontinuous Reception* (DRX) to conserve the power of MSs. DRX allows an idle MS to power off the radio receiver for a predefined period (called the *DRX cycle*) instead of continuously listening to the radio channel [10].

The UMTS DRX mechanism is realized through the *Radio Resource Control* (RRC) finite state machine exercised between the RNC and the MS [11]. There are two modes in this finite state machine (see Figure 2). In the RRC Idle mode, the MS is tracked by the core network without involving the UTRAN. When an RRC connection is established between the MS and its serving RNC, the MS enters the RRC Connected mode [12]. This mode consists of four states. If the MS obtains a dedicated traffic channel for the RRC connection, it enters the Cell DCH state. On the other hand, if the MS is allocated a common or shared traffic channel (i.e., the channel is shared by several MSs), it enters the Cell FACH state. The data communication activities can only be performed in these two states. In the Cell PCH state, no uplink access is possible, and the MS selects a Paging Channel (PCH) to monitor paging messages from the RNC. In the above three RRC states, the MS performs location update whenever it moves to a new cell (i.e., the radio coverage of a Node B). If the MS receives packets infrequently, the UTRAN may eliminate the cell update overhead by instructing the MS to move to the URA PCH state [13]. In this state, the MS performs location update for every *UTRAN Registration Area* (URA) crossing. In the Cell DCH and Cell FACH states, the MS receiver is always turned on to receive packets.

These states correspond to the *power active mode*. In the RRC Idle mode, Cell PCH and URA PCH states, the DRX is exercised to reduce the MS power consumption. These states/mode correspond to the *power saving mode*.

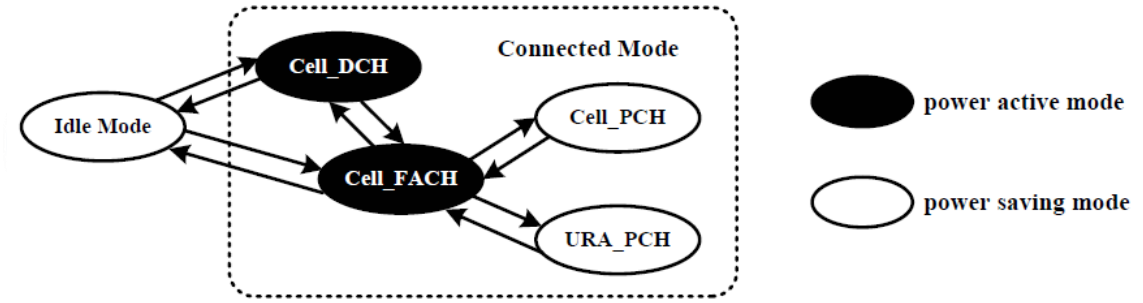

Figure 3.2: The RRC state diagram.

3.1.3. Smartphone power model for UMTS.

Power conservation in battery-operated mobile terminals is a serious consideration. It is obvious that the terminals can operate for a longer time on battery power if power consumption is reduced [14]. One approach to reduce the power consumption of mobile terminals is to place them into a state of low power consumption when the terminals are not communicating via radio channels.

The MS receiver activities are illustrated in Figure 3.3, and are described in terms of three periods:

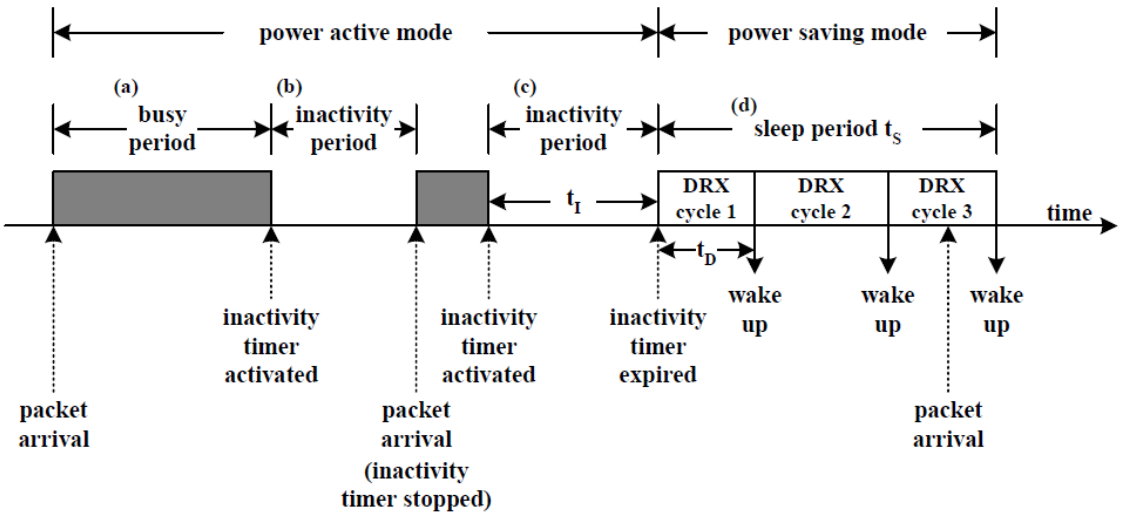

Figure 3.3: The timing diagram for the UMTS DRX mechanism [6].

The busy period**:** during packet transmission (i.e., the "server" is "busy"; see Figure 3.3(a)), the UMTS core network sends the packets to an MS through the RNC and Node B. The incoming packets are first stored in the RNC buffer before they are delivered to the MS. Since the MS is in the power active mode, the RNC processor immediately transmits packets in the *First In First Out* (FIFO) order [15].

The inactivity period: if the RNC buffer becomes empty, the RNC inactivity timer is activated (see Figure 3.3(b)). If any packet arrives at the RNC before the inactivity timer expires, the timer is stopped. The RNC processor starts to transmit packets, and another busy period begins. Note that the MS is in the power active mode in both the busy and inactivity periods, where the MS receiver is turned off [16].

The sleep period: if no packet arrives before the inactivity timer expires (see Figure 3.3(c)), the MS enters the power saving mode (see Figure 3.3(d)) and the MS receiver is turned off. The MS sleep period contains at least one DRX cycles. At the end of a DRX cycle, the MS wakes up to listen to the PCH. If some packets have arrived at the RNC during the last DRX cycle (i.e., the paging indicator for this MS is set), the MS starts to receive packets and the sleep period terminates. Otherwise, the MS returns to sleep until the end of the next DRX cycle [17].

3.2. LTE.

3.2.1. Introduction.

The evolving fourth-generation (4G) wireless technologies and especially long term evolution (LTE) of Universal Mobile Telecommunications System (UMTS), offer high bandwidth for data transfer.

The interface and radio architecture of the system LTE are completely new. These updates were called Evolved UTRAN (E-UTRAN). A major achievement of E-UTRAN has been to reduce

the cost and complexity of the equipment, because the control node (known as UMTS RNC) has been removed. Therefore, the control functions of radio resources, control of quality service and mobility have been integrated into the new Node B, called evolved Node B (eNB). All eNB are connected via an IP network and can communicate with each other using the SS7 signaling protocol over IP. The employed modulation schemes are QPSK, 16-QAM and 64-QAM [18]. The architecture of the new network protocol is known as SAE, where eNode is the one that manages network resources.

The Evolved Packet Core is connected to packet data networks in the outside world such as the internet, independents corporate networks or IP multimedia subsystems. The interfaces that connect the different parts of the system are denoted Uu, S1 and SGi as shown in the following figure:

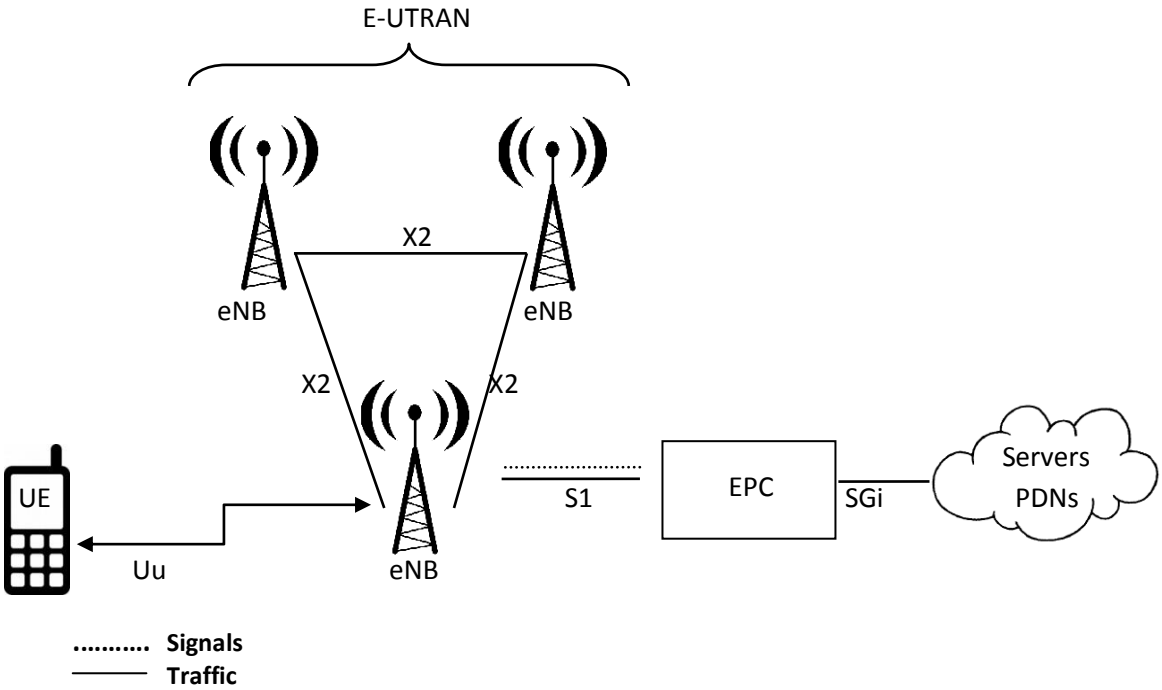

Figure 3.4: LTE architecture.

3.2.2. Discontinuous reception.

LTEs power efficient strategy exploits the concepts of DRX and Discontinuous Transmission (DTX). By using DRX, the terminal can turn the radio frequency modem into sleep mode for prolonged period either in order to extend battery life.

LTE has basically two RRC states, RRC_CONNECTED (device radio is in a high-power state, between 1000 and 3500 mW [19], while it either transmits data or waits for data, and dedicated radio resources are allocated by the radio network) and RRC_IDLE (device radio is in a low-power state, less than 15 mW and only listening to control traffic, no radio resources are assigned to the client within the carrier network. At RRC_CONNECTED state, UE can be in one of the three modes: Continuous Reception, Short DRX, and Long DRX. While at RRC_IDLE state,

UE is only in DRX mode. If UE is initially in RRC_IDLE state and receives or sends one packet, regardless of the packet size, a state promotion from RRC_IDLE to RRC_CONNECTED occurs with a relatively stable delay, similar to the promotion from IDLE to DCH/FACH in UTMS network. During this period, radio resources are allocated to the UE. After being promoted to RRC_CONNECTED, UE enters Continuous Reception by default and keeps monitoring the Physical Downlink Control Channel (PDCCH), which delivers control messages to UE. UE also starts the DRX inactivity timer T_i, which is reset every time UE receives or sends a packet. Upon T_i's expiration without seeing any data activity, UE enters the Short DRX mode. Discontinuous Reception (DRX) is adopted by LTE for UE to "micro-sleep" to reduce power consumption while providing high QoS and connectivity. DRX in RRC_CONNECTED and RRC_IDLE have similar mechanisms, but different parameter settings. A DRX cycle includes an On Duration during which the UE monitors PDCCH. UE rests for the rest of the cycle to save energy. The tradeoff between battery saving and latency is the guideline for determining the parameterization of DRX cycle. With a fixed On Duration, a longer DRX cycle reduces energy consumption of UE while increasing user-perceived delay, and a shorter DRX cycle reduces the data response delay at the cost of more energy consumption. Short DRX and Long DRX modes, having the same On Duration and differing in cycle length, are to meet these conflicting requirements.

When UE enters Short DRX, Short Cycle Timer T_{is} is started. Upon T_{is}'s expiration, if there is no data activity, UE witches to Long DRX; otherwise, UE goes back into Continuous Reception [20]. Every time UE enters Continuous Reception when there is any data transfer, UE starts the tail timer T_{tail}, which is reset every time a packet is sent or received. When T_{tail} expires, UE demotes from RRC_CONNECTED to RRC_IDLE and the allocated radio resource is released. Notice that T_{tail} coexists with Ti and T_{is}.

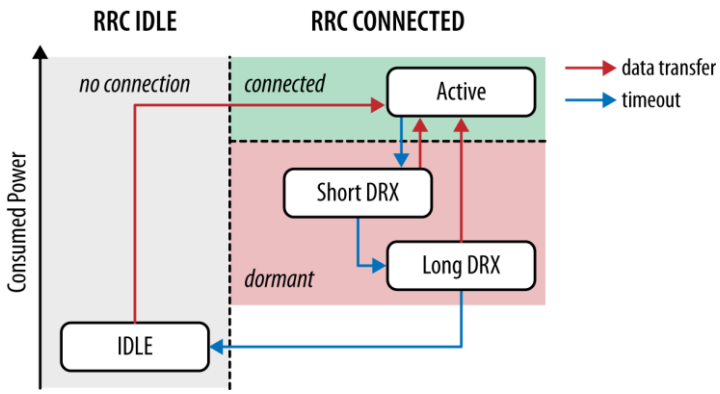

Figure 3.5: LTE RRC state diagram.

Essentially, capacity of PDCCH in the downlink depends on the number of multiplexed users per Transmission Time Interval (TTI) for scheduling radio frame resources. Since the availability of PDCCH resources is limited, the amount of multiplexed users per TTI is also restricted when TTI is fixed. Contrarily, by varying the TTI dynamically (i.e. increasing TTI when it is available) one may achieve the increased amount of multiplexed users per TTI. Longer TTI means increased amount of the data transmitted without increasing power consumption.

Thus, the TTI parameter in the layer should be configured so as to meet the performance requirement with minimize power consumption. A TTI with different size in the DRX Light and Deep Sleep mode could enhance the UE power consumption selected such that the power and resource savings are maximized.

3.2.3. Smartphone power model for LTE.

In this section the UE's power consuming physical layer components are examined one by one. The purpose is to determine how the components affect the total power consumption. Figure 6 shows the LTE physical layer components and the UE model parameters [21]. The envisioned UE model shall depend on receive (Rx) and transmit (Tx) power levels, uplink (UL) and downlink (DL) data rate, and RRC mode. In the following sections the parts in Figure 3.6 are examined to determine if and how they depend on the aforementioned parameters.

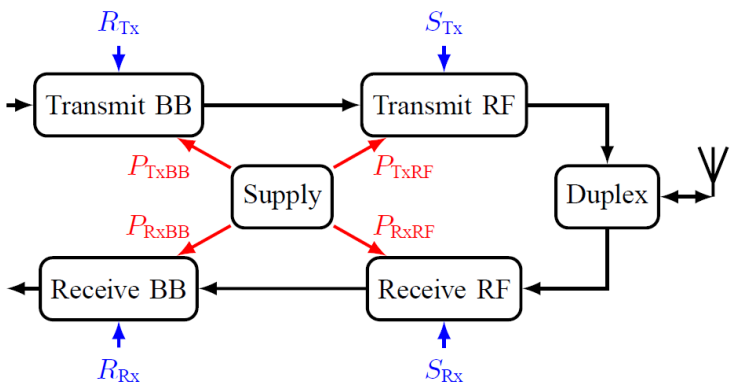

Figure 3.6: LTE UE physical layer.

- Transmit Baseband:
  In the LTE Tx baseband (BB) the main task is to turbo encode user data with Forward Error Correction codes. Turbo encoding relies on convolutional encoding and generates a bitstream with code rate 1/3. The Turbo encoding complexity scales linearly with the amount of data to encode which is set by the Transport Block Size (TBS) i.e. the UL data rate, but is independent of the UL Tx power.

- Transmit RF:
  In general the RF will not depend on the UL data rate, but when the modulation format is changed the Peak-to-Average Power Ratio (PAPR) is affected. This entails the PA will adjust its performance to comply with the Tx emission requirements in, such as the Adjacent Channel Leakage Ratio (ACLR), and this may affect the power consumption.

  The Tx RF will obviously depend on the UL Tx power. A single PA only has one output power level where it achieves its maximum energy efficiency, and therefore researchers develop methods to increase the efficiency at other output power levels.

These include the use of multiple PAs, supply voltage and bias switching, and the envelope tracking concept.

The Power Added Efficiency is expected to be stepwise increasing with output power as each of the methods is utilized.

- Receive RF:
  The Rx RF power consumption is expected to be independent of the DL data rate, but it will depend on the DL Rx power level. The reason is that the RF contains Gain Controls and Low Noise Amplifiers, which are used to obtain a certain signal level at the ADC. If the DL Rx power level is high the gain in the aforementioned circuits can be reduced, and they may be powered off, to reduce the power consumption.

- Receive Baseband:
  The majority of the Baseband processing tasks' complexity, e.g. channel estimation and equalization, is independent of the DL data rate. To decode the received user data the UE applies turbo decoding, which is an iterative algorithm and the most computational complex task in the digital BB. To support the high data rates of LTE a highly parallelized turbo decoder architecture is required. The complexity and thus the power consumption scale linearly with DL data rate.

3.2.4. Comparison with UMTS.

In the 3G state machine, the power drain in the DCH state is basically constant for all files. In LTE, the power drain in the Continuous Reception state varies depending on the throughput. Small files keep the power low, but as the throughput increases, the power gets even higher.

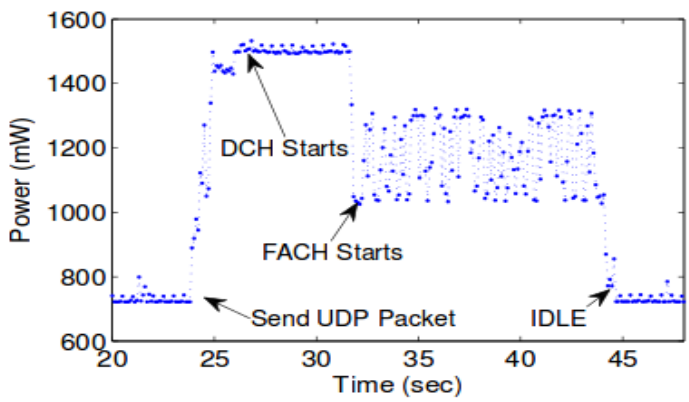

Figure 3.7: Power states of 3G.

The LTE radio states drain slightly more power than their counterparts in 3G, because the tail states (Short DRX and Long DRX) stay at the higher base power [22], while much of the 3G tail is in the FACH state which uses half power.

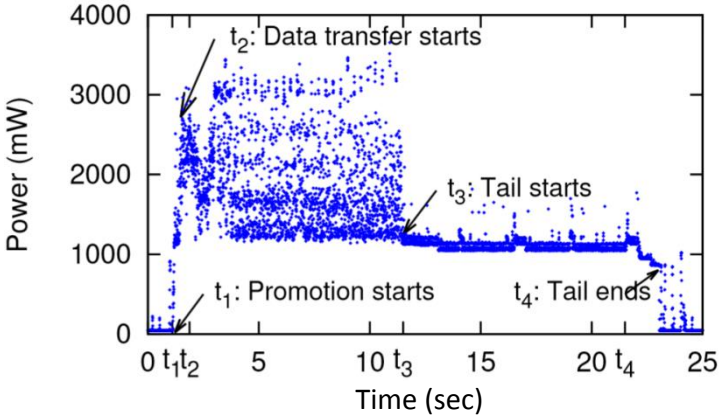

Figure 3.8: Power states of LTE.

So LTE causes a larger energy drain for the same amount of content due to the high power used in the Long DRX tail state, ergo LTE is less energy efficient during idle state and for transferring smaller amount of data [23]. One possible reason for LTE's higher power states is that devices must incorporate multiple-input and multiple-output (MIMO) to support LTE network.

However, for bulk data transfers, LTE is more efficient than UMTS due to high throughput for LTE, so the time in Continuous reception (T_i) is significantly lower.

Chapter 4.

The Measurement setup.

4.1. The hardware.

4.1.1. Introduction.

The first step to measure the energy consumed by a Smartphone when you is using a data connection, is preparing the necessary hardware. A USB modem that works with a SIM card which acts as a Smartphone is needed. This modem will be connected via USB to a Power Meter tool that in turn will be connected to a computer through the serial port to collect data using a software. This scheme is shown in the following figure:

Server Client

Figure 4.1: Scheme of the components used.

The following will explain in detail the two major components: the power meter and the USB modem.

4.1.2. USB Power Meter.

This device allows taking measurements of another USB device. The device consists of two Printed Circuit Boards: the first PCB has the microcontroller with sensing circuits and the second contains the OLED display and driver. The left side of OLED display will show the instantaneous bus voltage, shunt voltage drop, device voltage, and current usage with an update interval of 100ms. The right side will display a short term graph of the last minute of current usage.

Doing a verification test, it can be seen that the error rate of energy consumption was below than 1%.

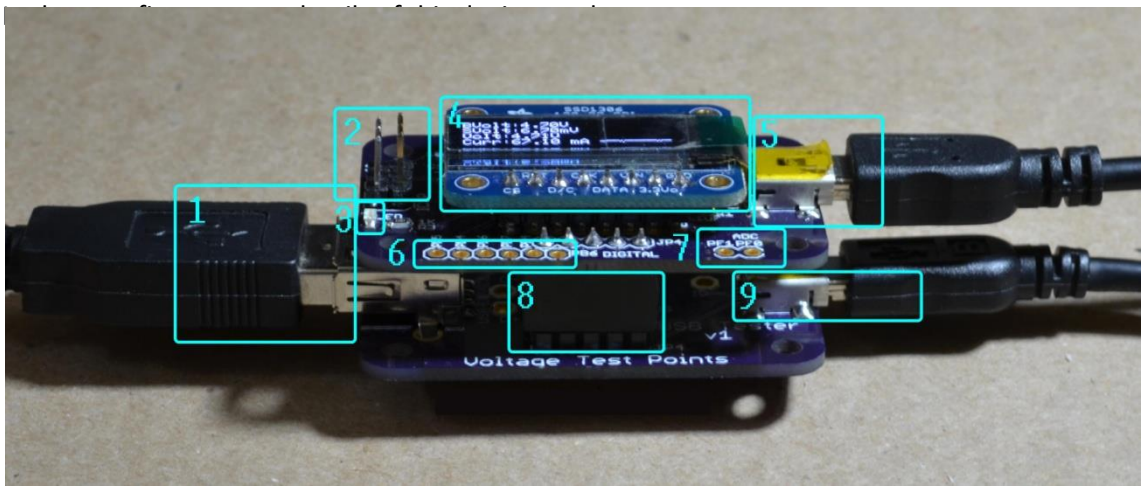

Figure 4.2: Power Meter.

The numbers in the figure correspond to the following parts:

1. USB A connection to measuring device.
2. ICSP programming headers. Above these headers is the RX/TX header.
3. LED for current warning set point.
4. OLED display which shows readout of values on the left and a mini graph on the right.
5. USB B mini connection to computer for data logging and uploading a new firmware.
6. Unused Digital GPIOs.
7. Unused ADC GPIOs.
8. Connection to USB Tester, there is another on the top side.
9. USB B mini connection to computer or power source.
10. Not visible is a mode button on the backside.

In the appendix A, more information about this device can be found.

4.1.3. USB Modem.

For acting as a Smartphone, a USB modem of Huawei brand has been used, in particular the E-397 model, which is compatible with both UMTS and LTE technologies.

The drivers and the firmware were updated to the last version for guaranteeing the better operational quality of the device.

The energy consumed by this device at rest is 3.6 mJ.

In the appendix B, it can be found more features about this device.

Figure 4.3: USB modem.

4.2. The software.

4.2.1. Introduction.

Once all the hardware is ready, now is the turn of the software. This has been the main part of the project and has taken longer: implementing a Java program that performs the following functions described in this scheme:

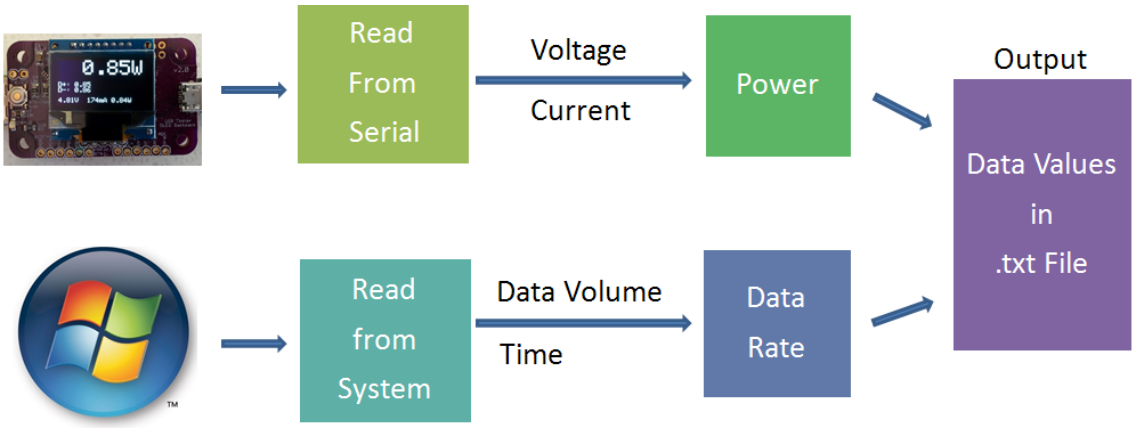

Figure 4.4: Scheme of the software behavior.

First, the program must be able to read from the Power Meter hardware the values corresponding to the voltage and current of the USB modem. Once they are stored, it has to multiply them for deriving the power consumption.

Moreover, the program has to be able to pick from the system (in this case Windows) the volume of data that has been consumed. Also the system itself has to take the time in which each measurement occurs. Once it has these two values, it has to divide the volume between the time to get the data rate. Once it already has all the values, it saves them to a text file, allowing easier exportations of these values to programs such as Matlab. These data are as follows: voltage (in Volts), current (in mAmpers), power (in mWatts), energy (in Jules), uploaded data volume (in KBytes), downloaded data volume (in KBytes), total data volume (in KBytes) and Unix time (in seconds).

It is noteworthy that the program is designed to perform three types of measurements, which are the most commonly used when using a Smartphone: videostreaming, web traffic and email sending.

Also it has a graph that shows the power consumption in function of time.

4.2.2. Graphical interface.

The following figure shows the appearance of the graphical interface of the program and each of its parts are explained in more detail:

1. This is the graph that shows the power consumed (in mWatts) by the USB modem in function of time.
2. This box is for videostreaming. The address of where the video is hosted can be written here, and plays the video with the video player that is set by default.
3. Here the video resolution is selected. The options are: the best, the medium and the worst resolution.
4. The time (in hours, minutes and seconds) that is wanted to be measured can be indicated here. If a time greater than the duration of the video is written, the video will loop until the time runs out. If the duration of the measurement is not known in advance, the “Loop” option can be clicked.
5. This part is for emails. This box is for writing the subject corresponding to the email.
6. Here the body of the message of the email can be written.
7. The address of the sender of the email is written here.
8. The email address of the receiver is written in this box.
9. Here the password of the account from which the email is sent is written.
10. The number of emails you want to send in a row is written here. The minimum is 1.
11. This part is for web browsing. The address of the web page that is wanted to access is written here. The program will open it with the default web browser.
12. Here it can be chosen the communications port which the USB modem is connected to, in case that more than one device is connected.

13. These are the buttons Start and Stop. To start measuring it must be pressed Start and to finish measuring, the button Stop must be pressed. If time is specified in the box 4, there is no need to press Stop because the program will stop alone.
14. This shows whether the device is connected, disconnected or if there is some kind of connection error.
15. Here it shows the number of measures it has been taking the program from being clicked Start.
16. Here the summation is shown (in Jules) of the total energy consumed by the USB modem.
17. The kind of measurements can be chosen here: email sending, web browsing or videostreaming.
18. Finally, if the button File is clicked, it saves in a text file the data that has been collected since the Start button was pressed.

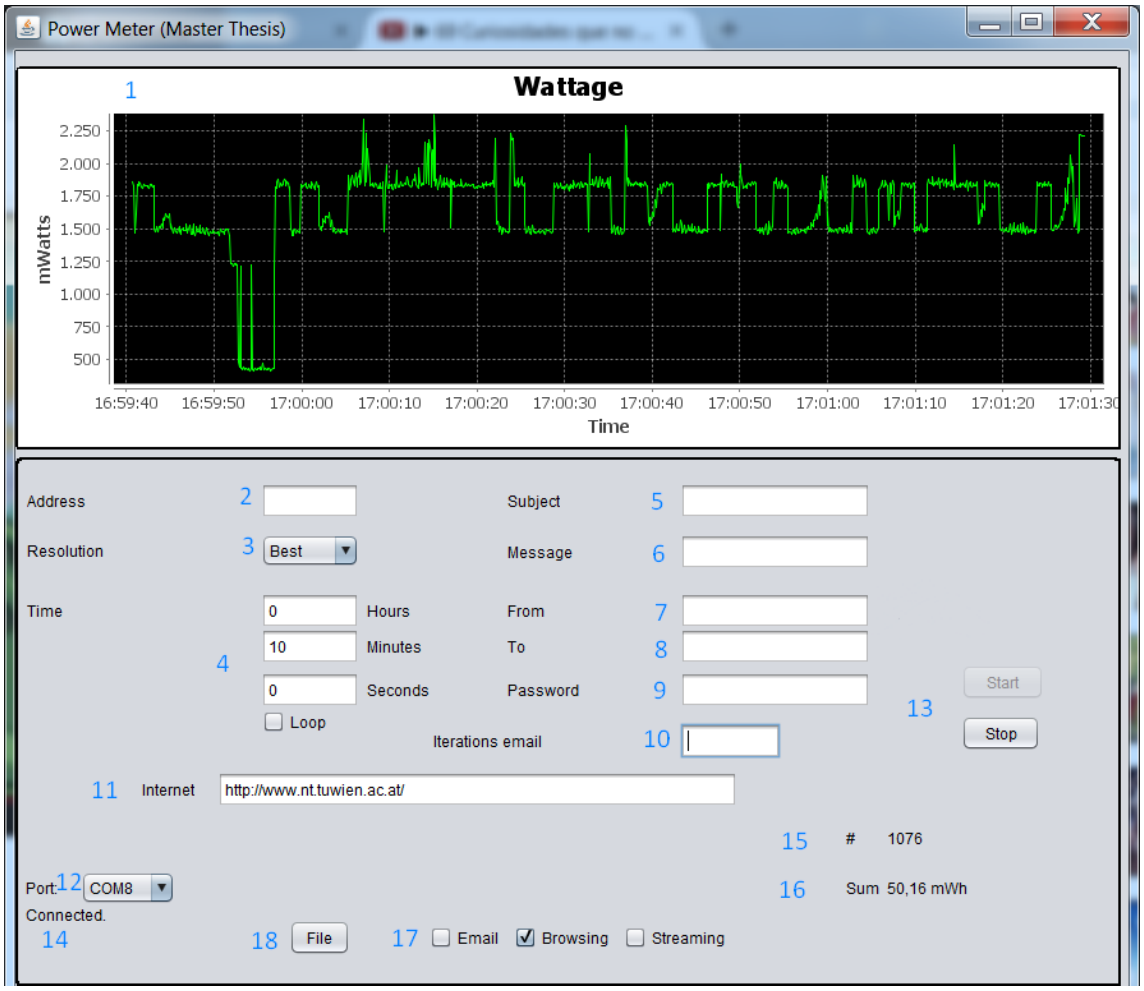

Figure 4.5: Software graphical interface.

Chapter 5.

The measurements.

This section will describe first the different scenarios that have been used to conduct the measures and secondly the results obtained.

5.1. The scenarios.

Three types of measures have been conducted and each of them using UMTS and LTE technologies and then considering the impact of link quality:

5.1.1. Web traffic.

This scenario is divided in two parts: Uplink and Downlink.

For simulating web traffic, it has been used the platform D-ITG (Distributed Internet Traffic Generator) that is capable to produce traffic at packet level accurately replicating appropriate stochastic processes for both N_p (*number of Packets*) and S_p (*Packet Size*). The following figure shows the scheme of how would be that packet traffic, where PC are the packet calls, IT is the Packet inter-arrival time and RT is the reading time between PCs.

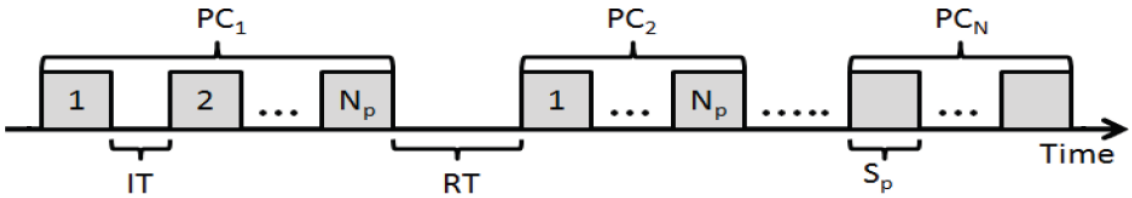

Figure 5.1: Web Traffic Model.

In this scenario, a sweep has been conducted, in both cases Uplink and Dowknlink, in which have been changed the size of each packet, starting from 200 bytes to 3200 bytes using powers of two and also the number of packets has been changed from 10 to 1000 packets per seconds using powers of ten. Or if it is expressed in bit rate, the sweep goes from 2 KBytes/s to 3.2 MBytes/s (from 16 kb/s to 25.6 Mb/s). The duration of each measurement is two minutes.

5.1.2. Videostreaming.

For conducting this part, a video from twitch.com has been measured for thirty minutes using three kinds of resolution: 720p, 480p y 360p. The video player used to play the video has been VLC Media Player and to introduce the commands in the command console it was used the software Livestreamer so all the process could be automatized.

5.1.3. Email sending.

To carry out this part, 1, 5 and 10 emails in a row were sent, with a subject whose size is 10 Bytes (ten letters) and with a message whose size is 10 Bytes too (the same ten letters). The sender server was Gmail and the receiver server was Hotmail.

5.2. Results.

Here are shown the results of the corresponding scenarios from the previous section.

In each of the graphs, it can be seen the histogram corresponding to the empirical probability density function (ePDF) of the power data that have been collected by the software. These graphs have been processed using Matlab.

As there are hundreds of measurements, here are shown only the most important. More results can be seen in the appendix.

5.2.1. Web traffic.

With these results it can be observed that more energy is consumed in the following cases:

- High data rates.
- Uplink.
- LTE technology.

Uplink.

UMTS.

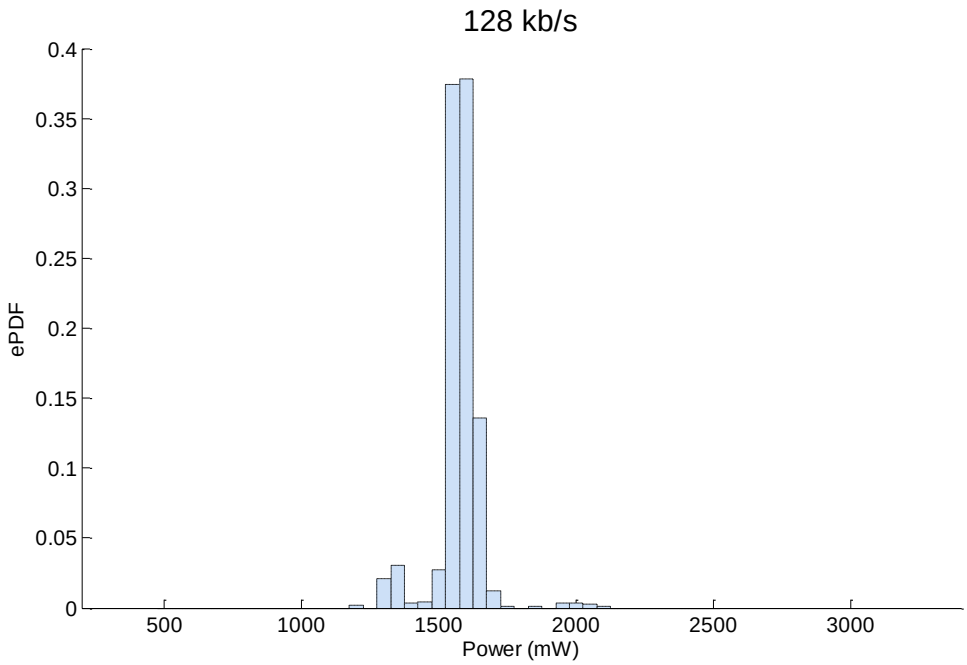

Figure 5.2: Uplink in UMTS at 128 kb/s.

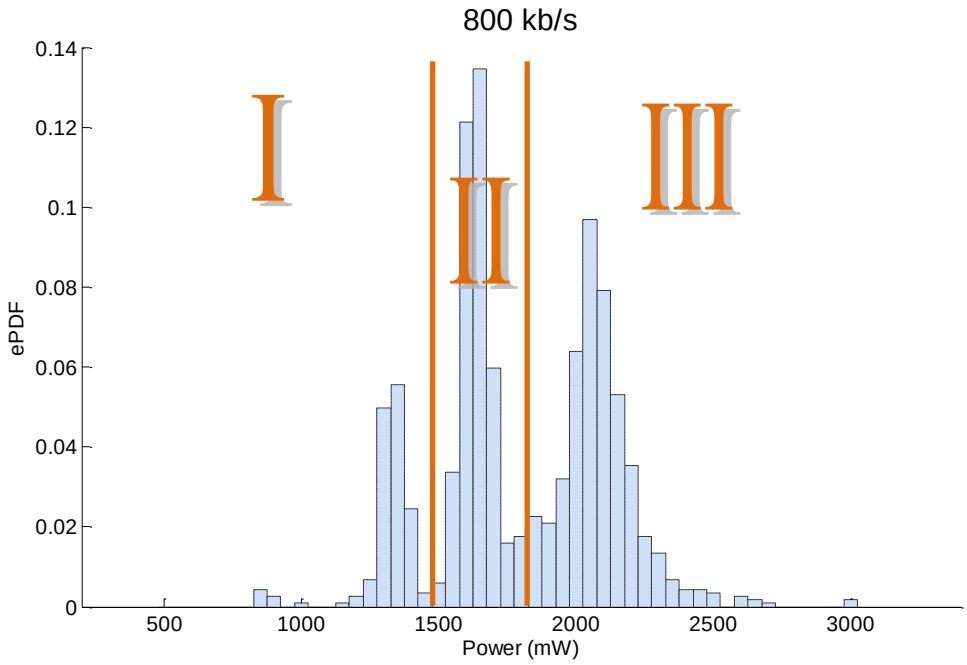

Figure 5.3: Uplink in UMTS at 800 kb/s.

In the chart above it can be clearly seen the three different states of the state machine for UMTS: I is IDLE, II corresponds to CELL_FACH and III belongs to CELL_DCH.

LTE.

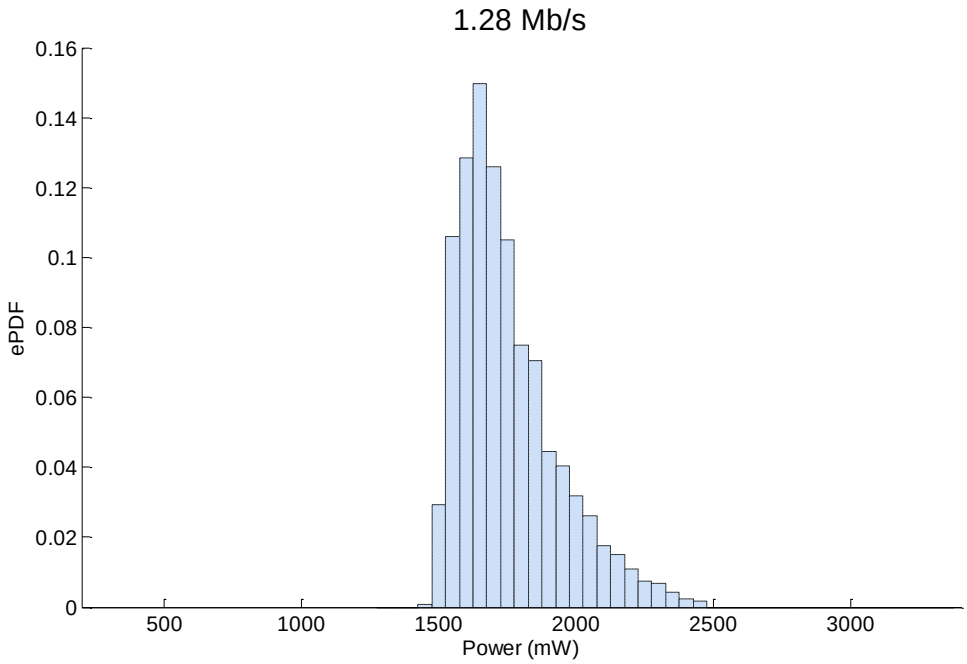

Figure 5.4: Uplink in LTE at 1.28 Mb/s.

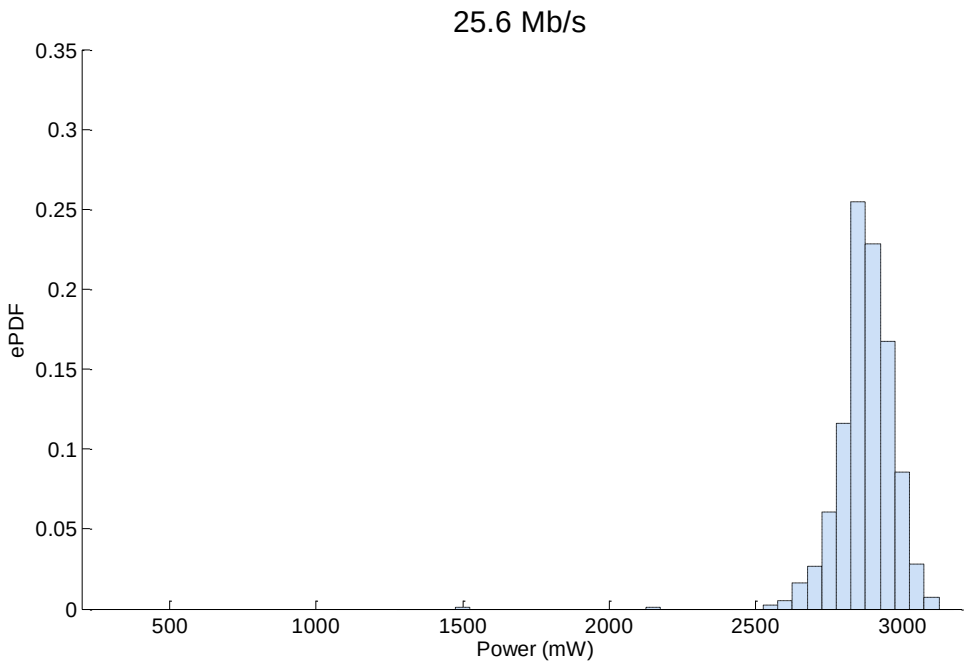

Figure 5.5: Uplink in LTE at 25.6 Mb/s.

Downlink.

UMTS.

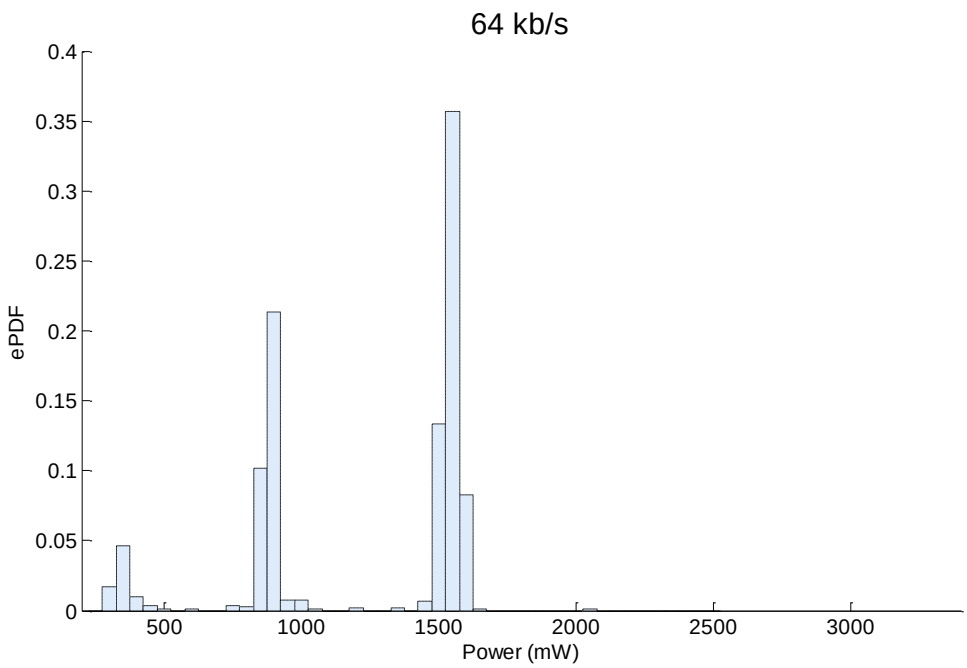

Figure 5.6: Downlink in UMTS at 64 kb/s.

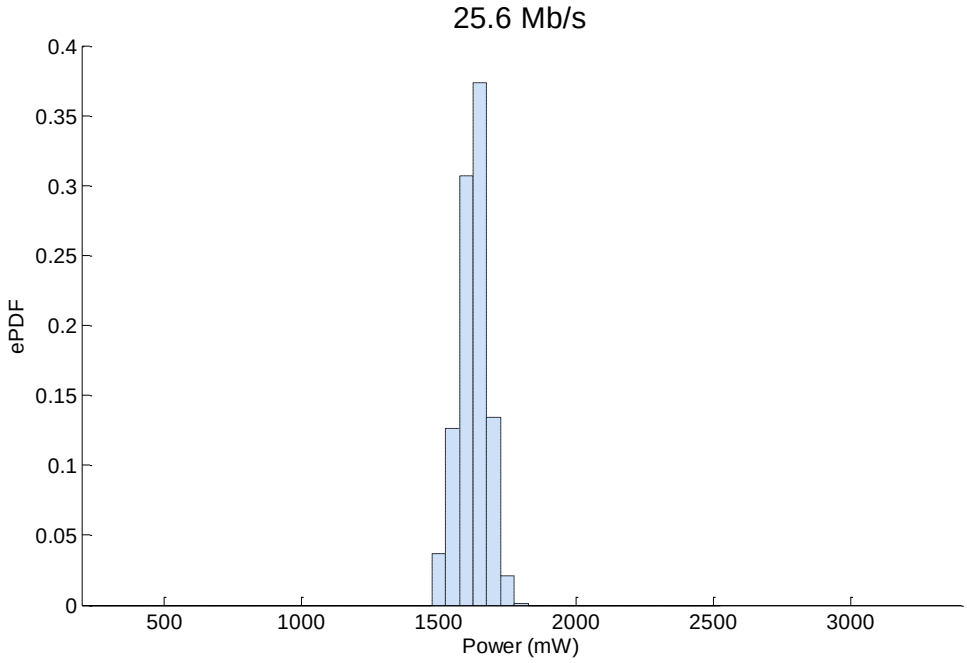

Figure 5.7: Downlink in UMTS at 25.6 Mb/s.

LTE.

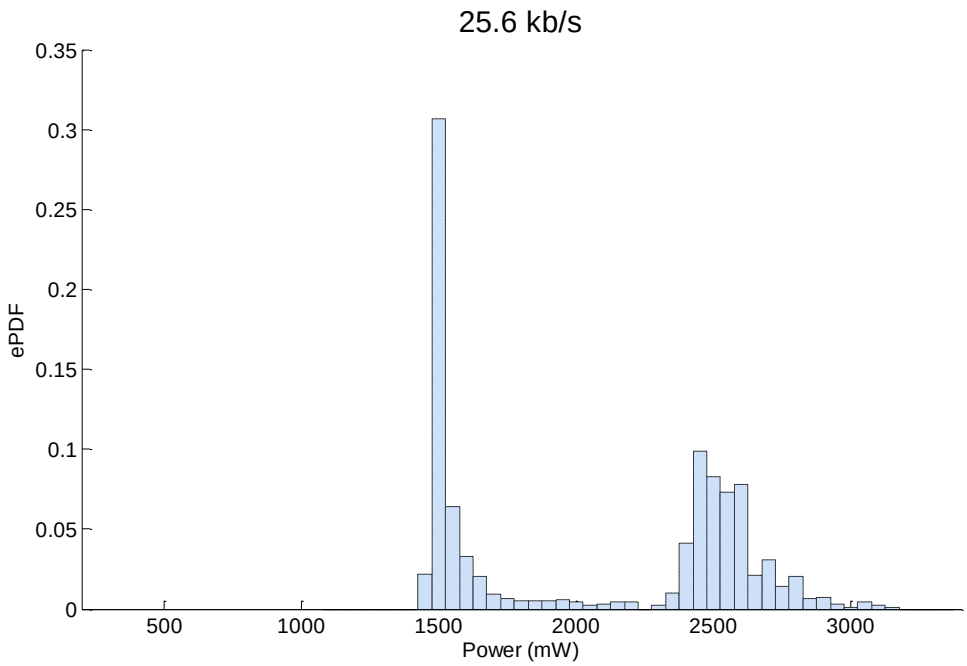

Figure 5.8: Downlink in LTE at 25.6 kb/s.

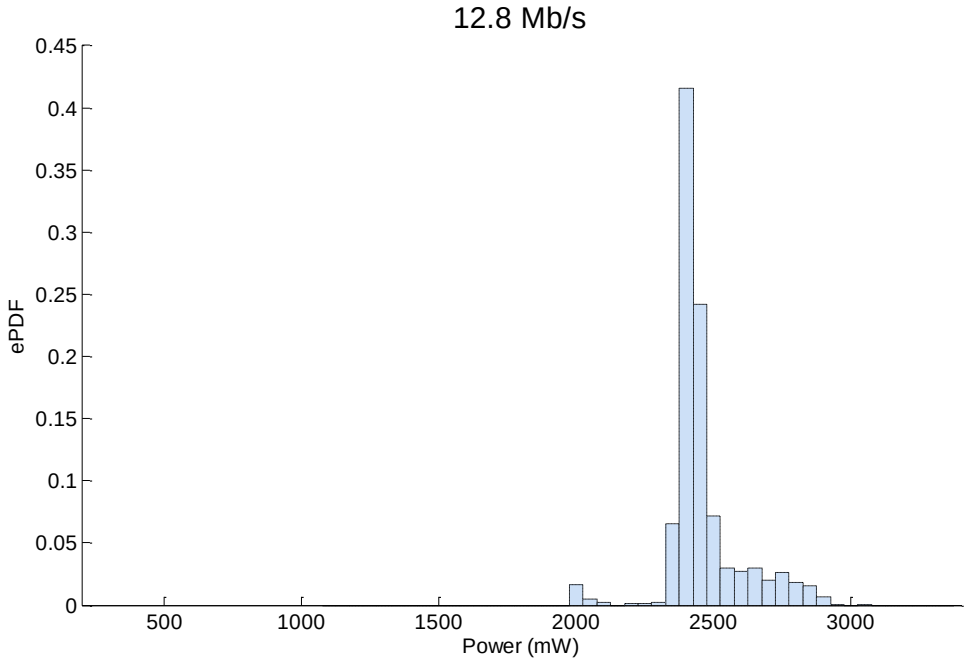

Figure 5.9: Downlink in LTE at 12.8 Mb/s.

5.2.2. Video.

It can be seen that more energy is consumed in the following cases:

- High resolutions: they correspond to high data rates and like in the previous graphs, the device consumed more energy with high data rates.
- LTE.

Also notice that is consumed more energy for video streaming than for traffic download. That is because in video streaming there is a component of uploading when some packets have not arrived and the protocol has to request them again.

UMTS.

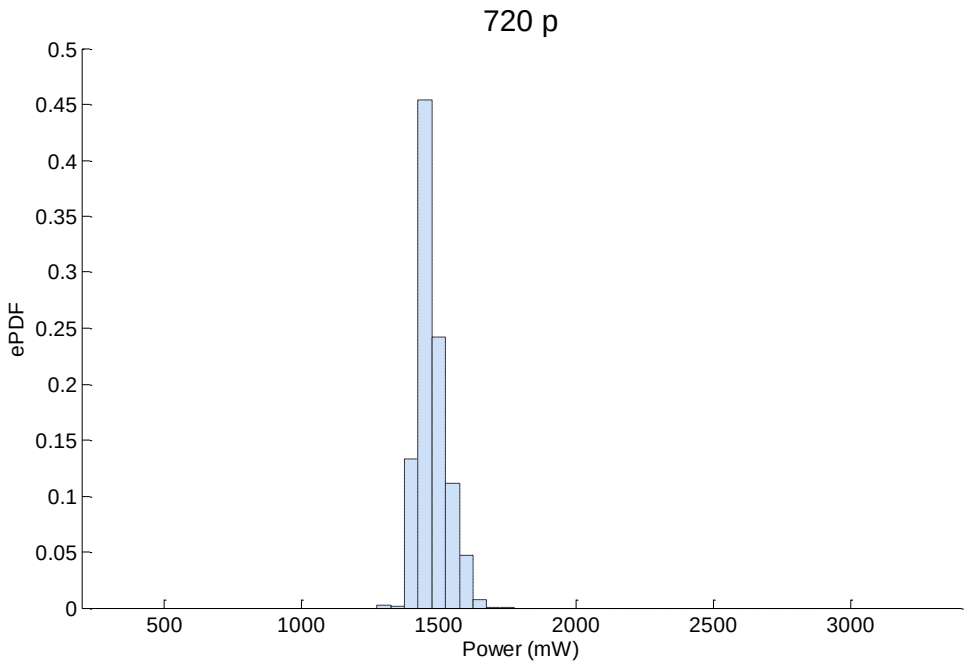

Figure 5.10: Videostreaming in UMTS at a resolution of 720p.

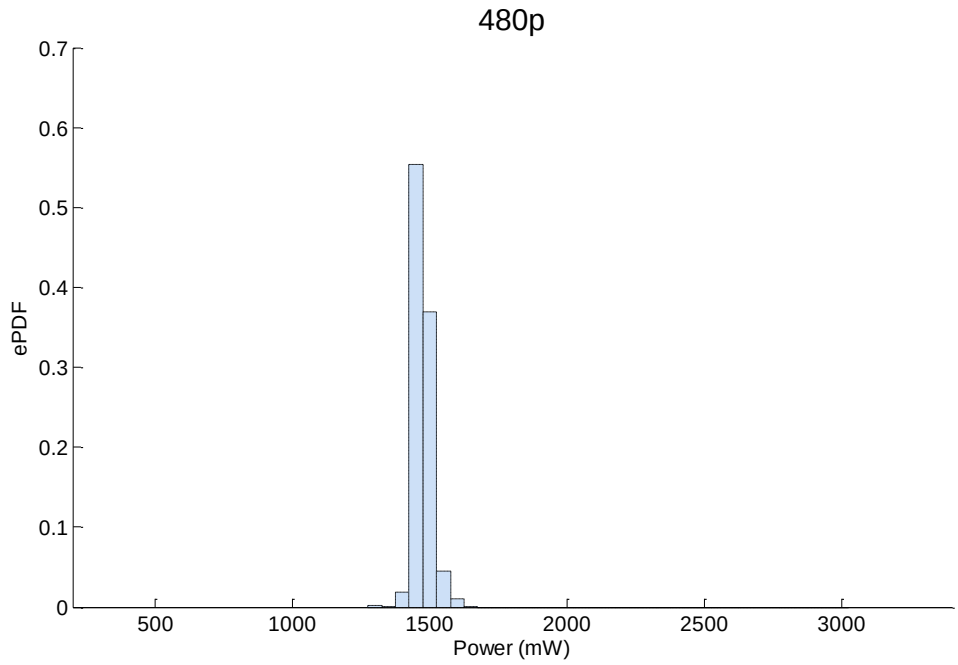

Figure 5.11: Videostreaming in UMTS at a resolution of 480p.

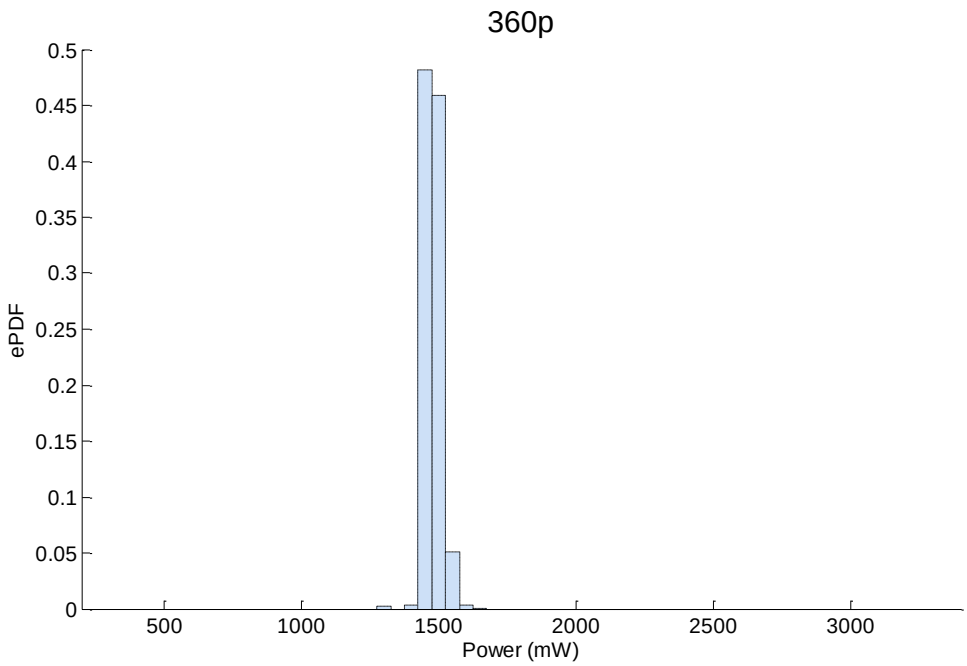

Figure 5.12: Videostreaming in UMTS at a resolution of 360p.

LTE.

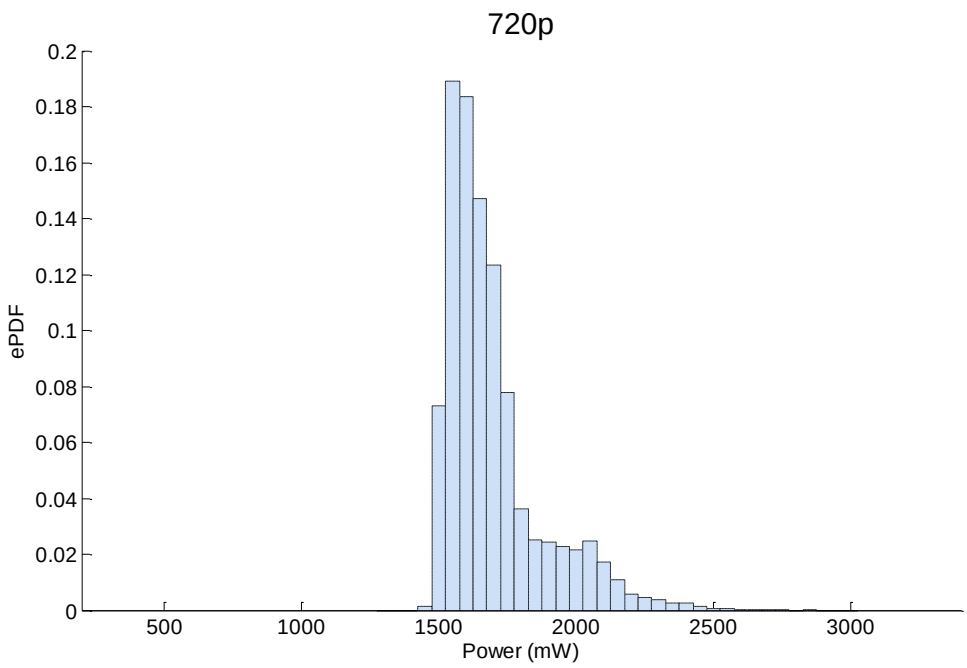

Figure 5.13: Videostreaming in LTE at a resolution of 720p.

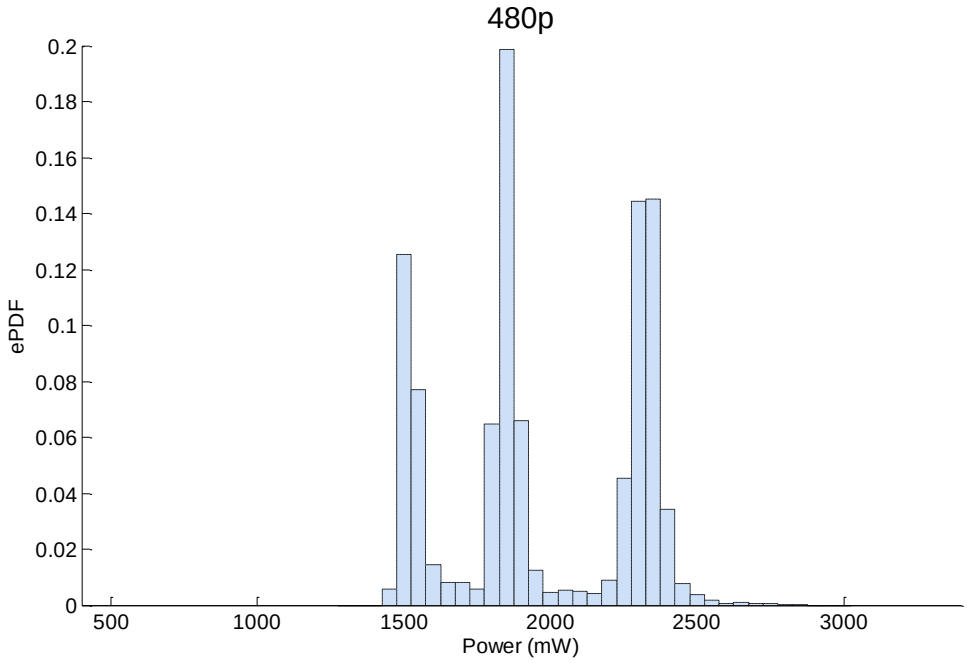

Figure 5.14: Videostreaming in LTE at a resolution of 480p.

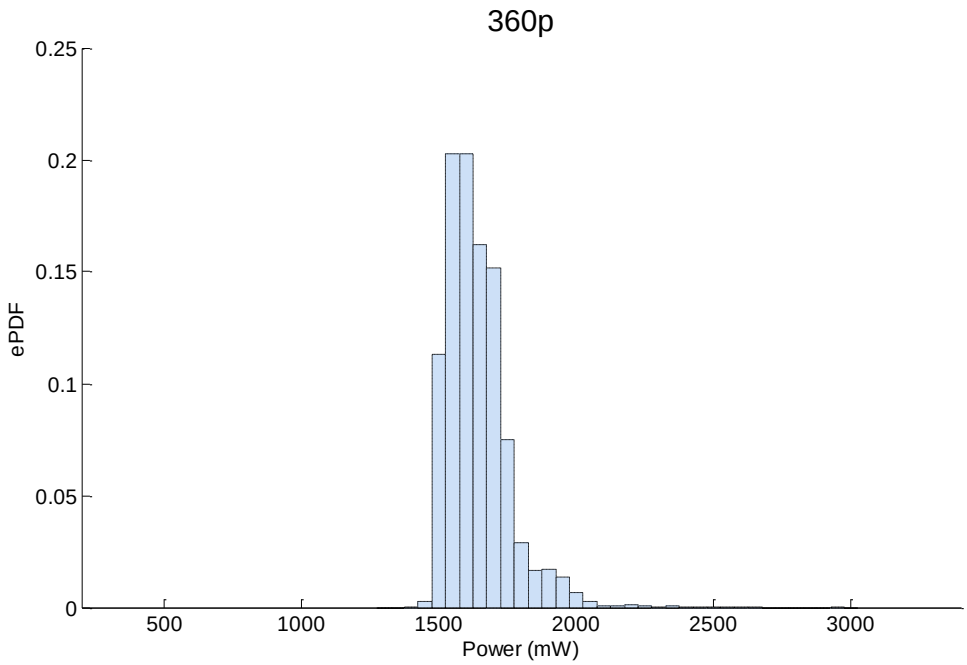

Figure 5.15: Videostreaming in LTE at a resolution of 360p.

5.2.3. Email.

In each technology, the energy used to send 1, 5 or 10 emails is approximately the same because the size of data sent is small.

One can also observe that the device consumes more power in LTE than in UMTS.

UMTS.

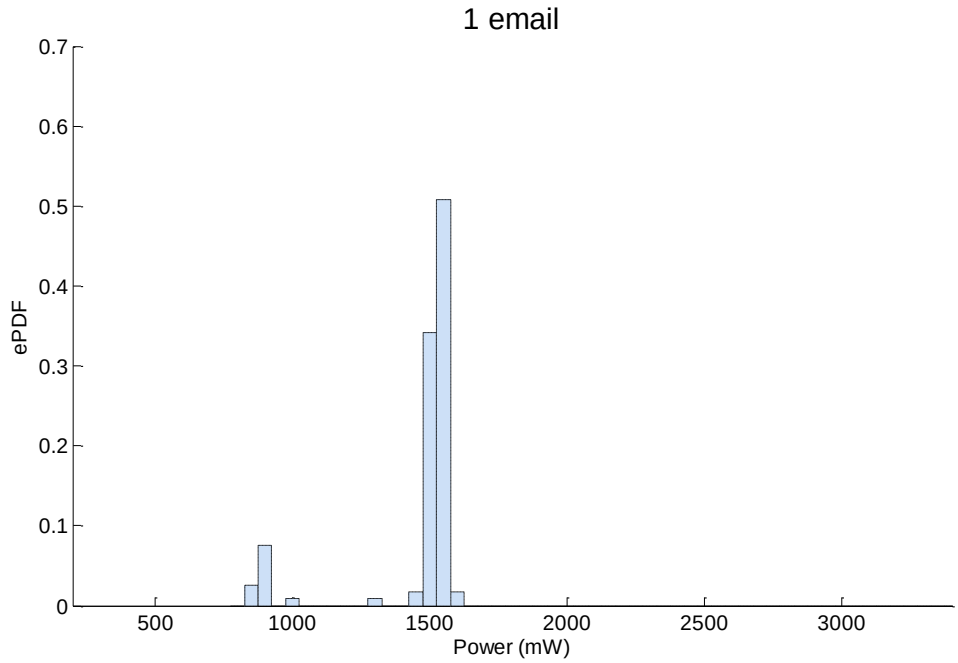

Figure 5.16: Sending in UMTS 1 email.

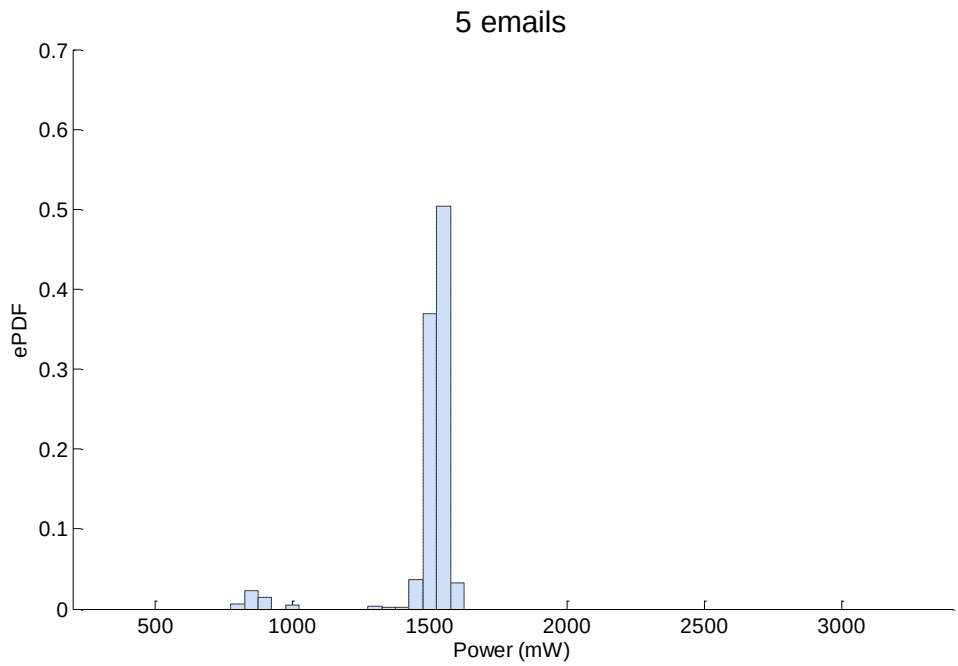

Figure 5.17: Sending in UMTS 5 emails in a row.

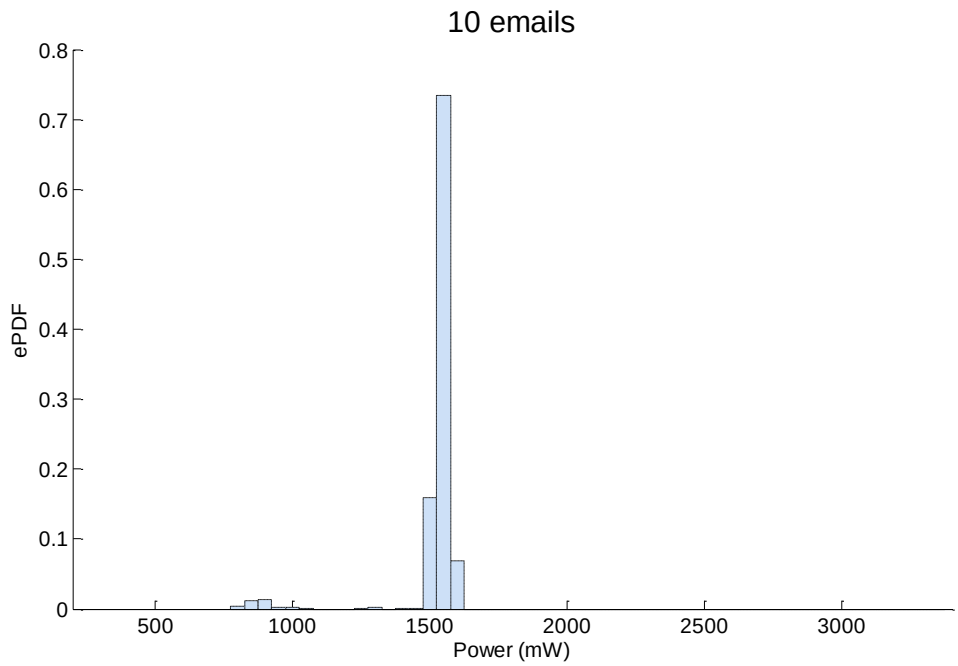

Figure 5.18: Sending in UMTS 10 emails in a row.

LTE.

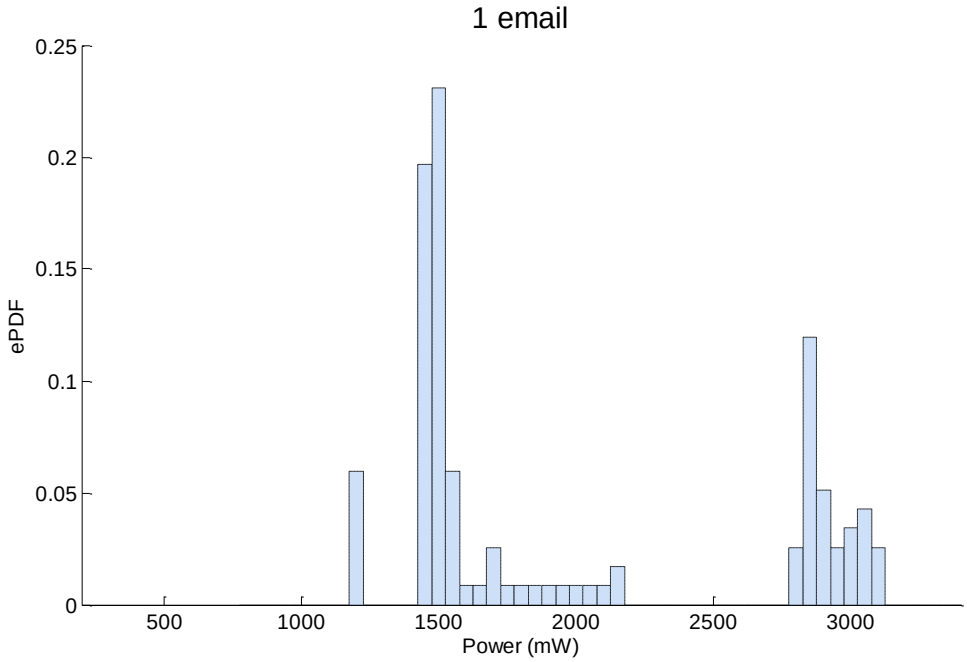

Figure 5.19: Sending in LTE 1 email.

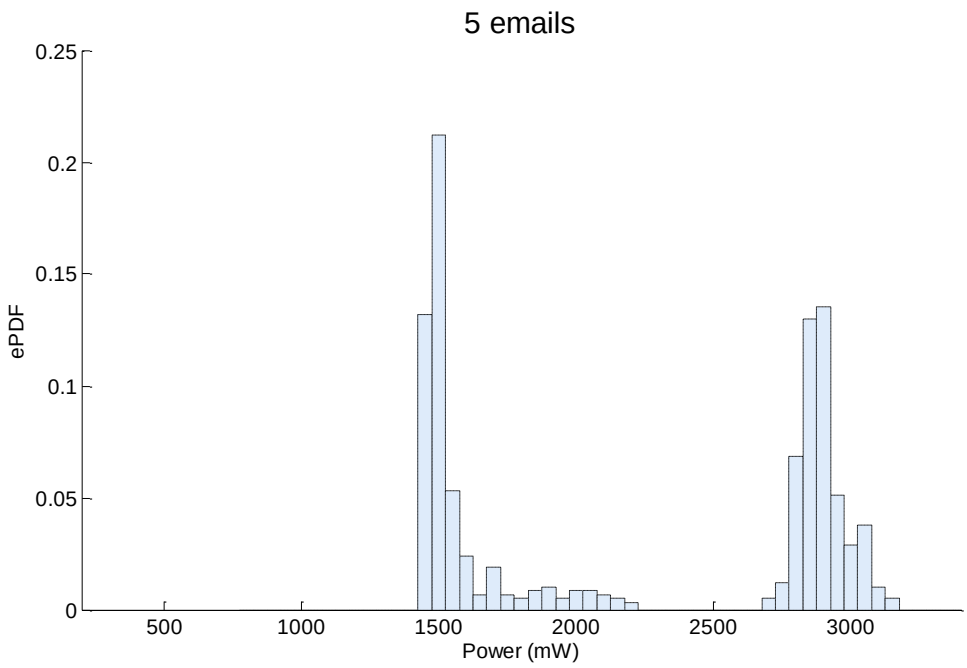

Figure 5.20: Sending in LTE 5 emails in a row.

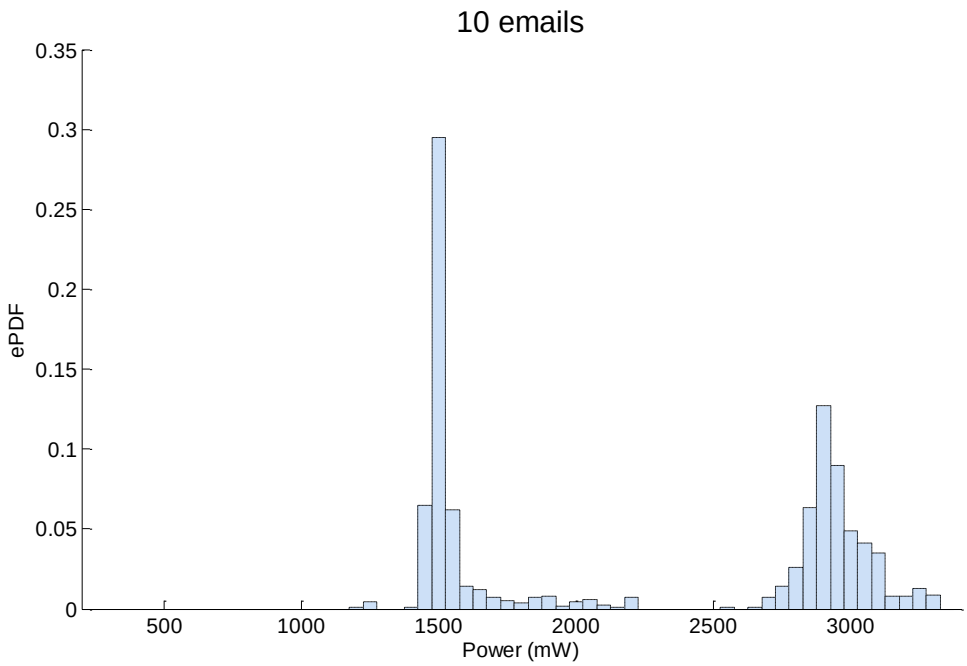

Figure 5.21: Sending in LTE 10 emails in a row.

5.3. Impact of link quality on power.

Once collected all the results, the author of this thesis realized that the USB modem consumed more power than what was supposed to consume. This is due to link quality since the worse the coverage, the more power the device needs to send and receive data because more packets are lost and they have to be requested again. As the measurements were taken with the Modem in the laboratory, the quality of the signal was 55%. For obtaining more accurate measurements, all the measurements were performed again with the modem outside the window, achieving improvements up to 20dB because signal quality raises until 90%. These were the new results.

5.3.1. Web traffic.

Uplink.

UMTS.

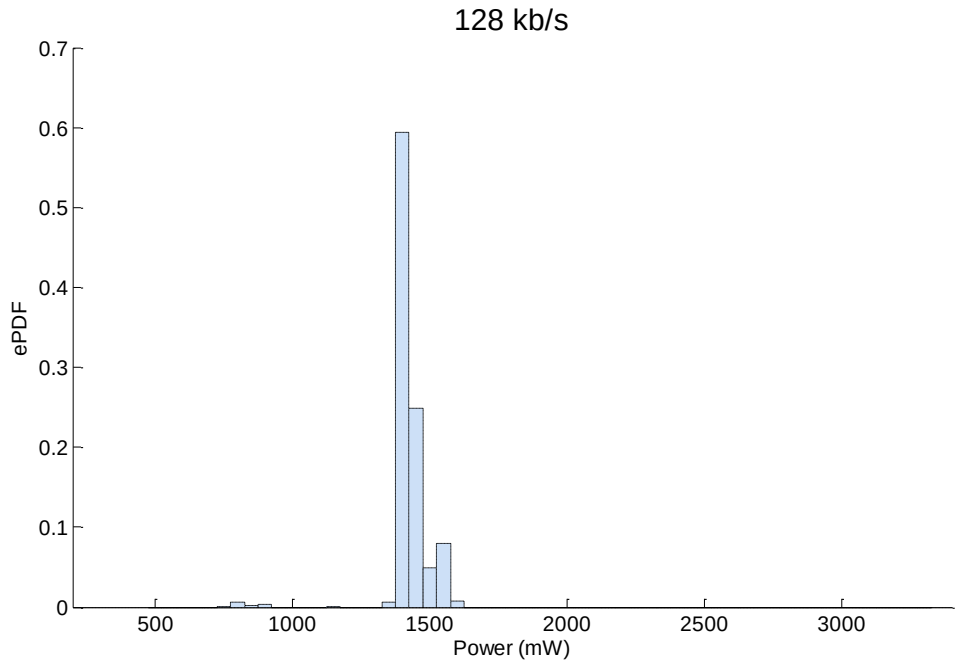

Figure 5.22: Uplink in UMTS at 128 kb/s with 90% of quality signal.

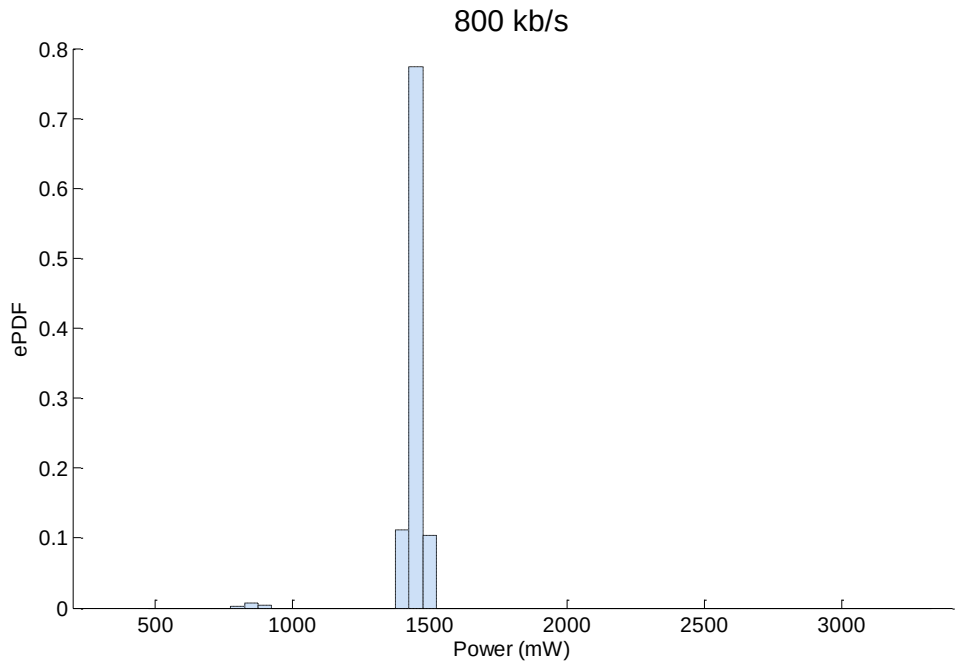

Figure 5.23: Uplink in UMTS at 800 kb/s with 90% of quality signal.

LTE.

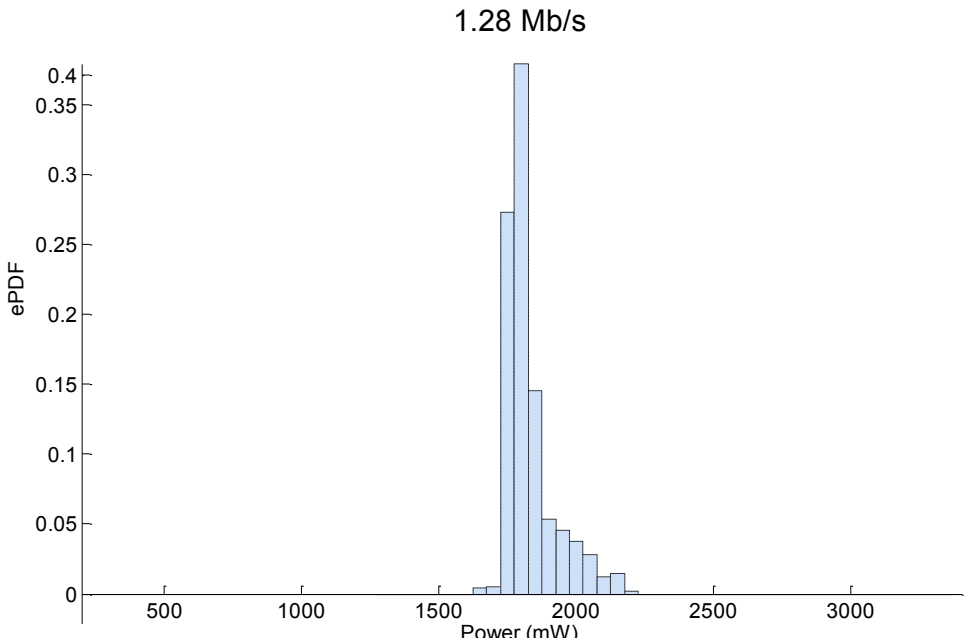

Figure 5.24: Downlink in LTE at 1.28 Mb/s with 90% of quality signal.

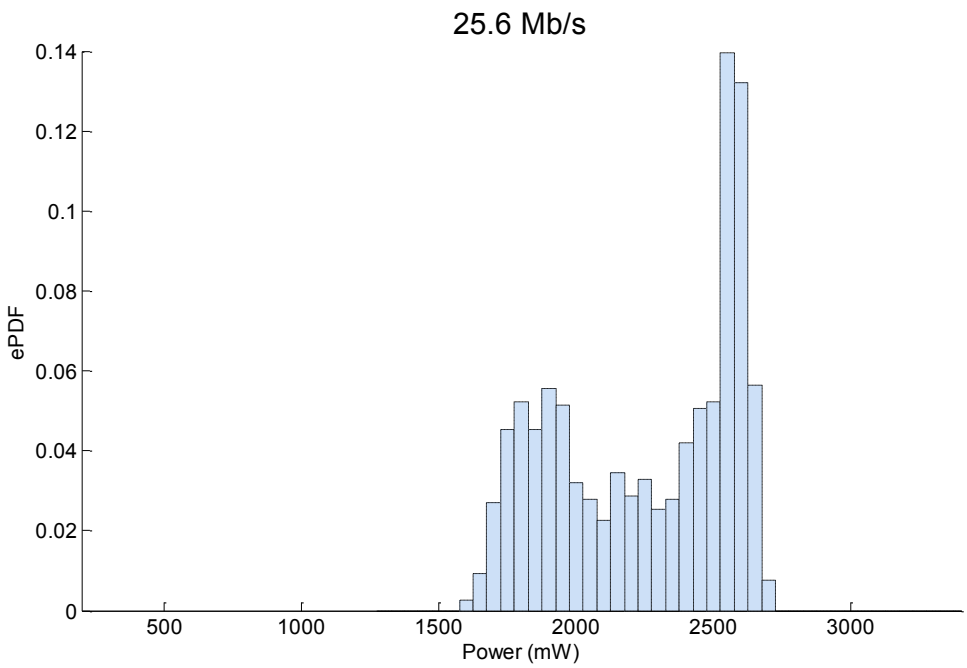

Figure 5.25: Downlink in LTE at 25.6 Mb/s with 90% of quality signal.

Downlink.

UMTS.

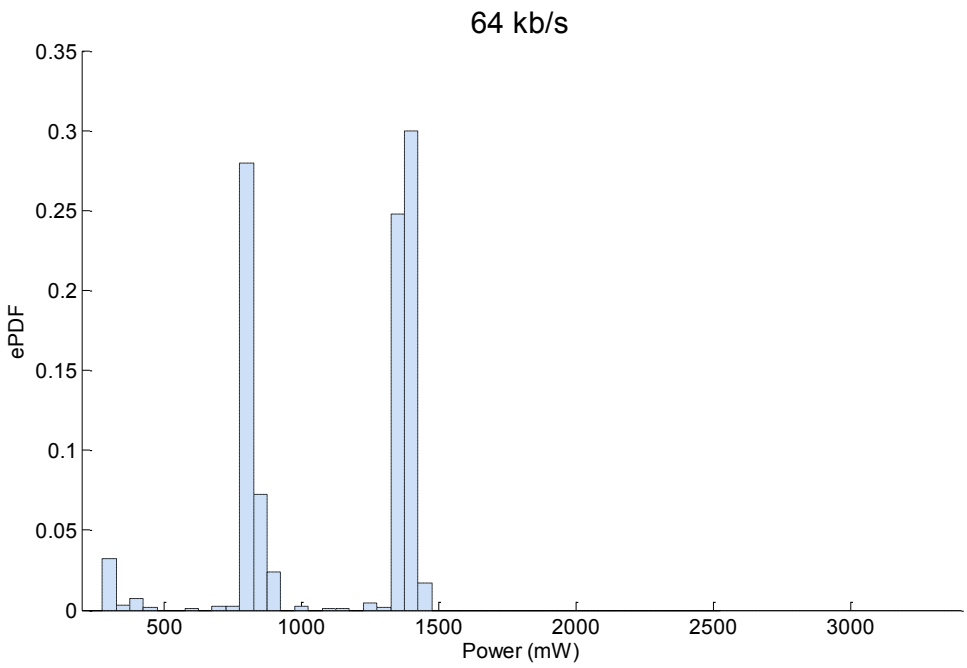

Figure 5.26: Downlink in UMTS at 64 kb/s with 90% of quality signal.

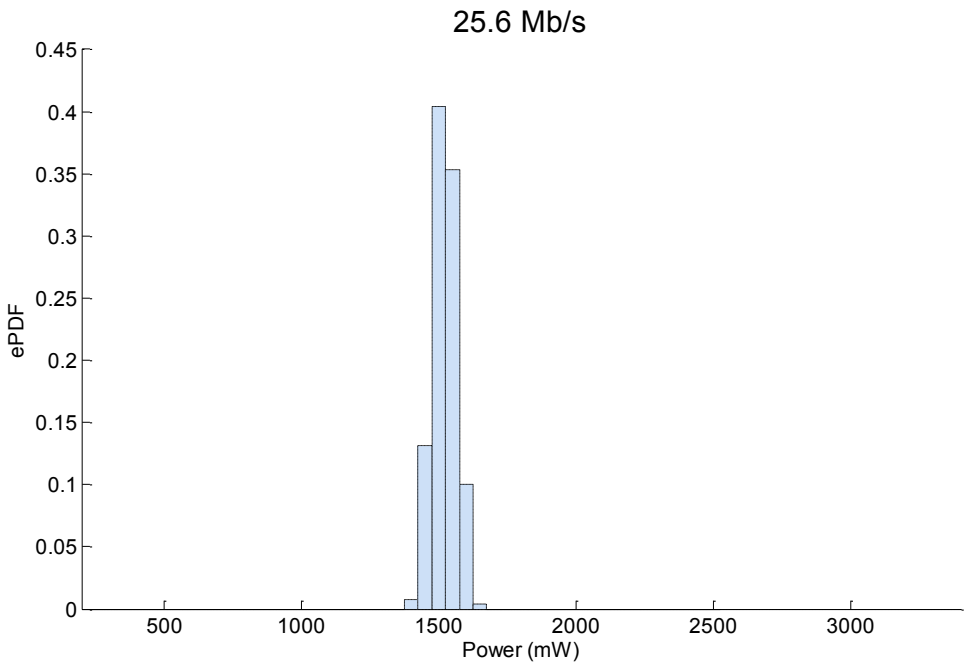

Figure 5.27: Downlink in UMTS at 25.6 Mb/s with 90% of quality signal.

LTE.

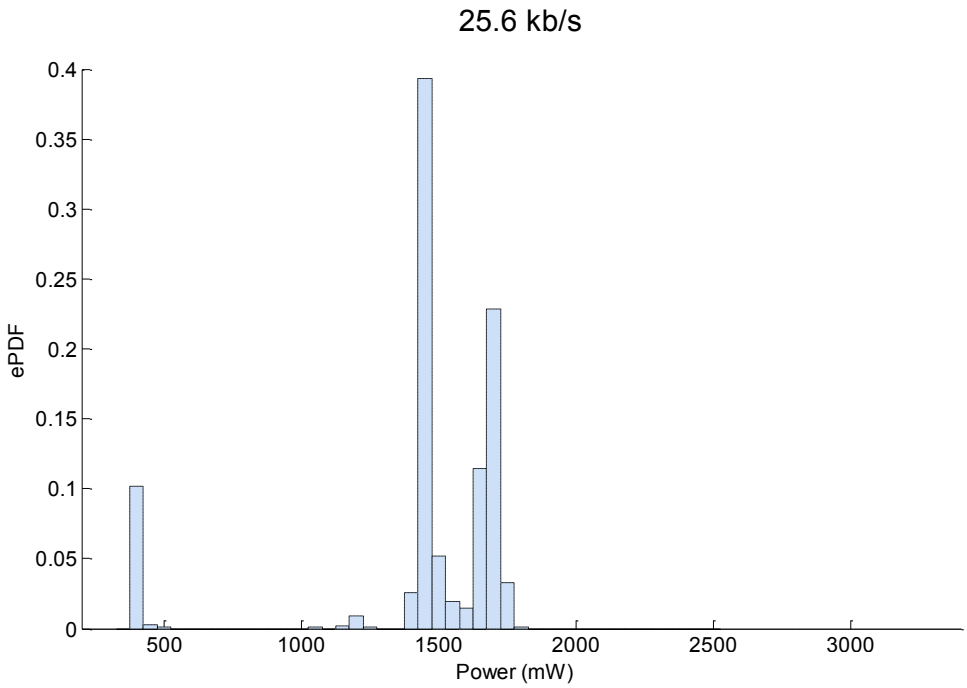

Figure 5.28: Downlink in LTE at 25.6 kb/s with 90% of quality signal.

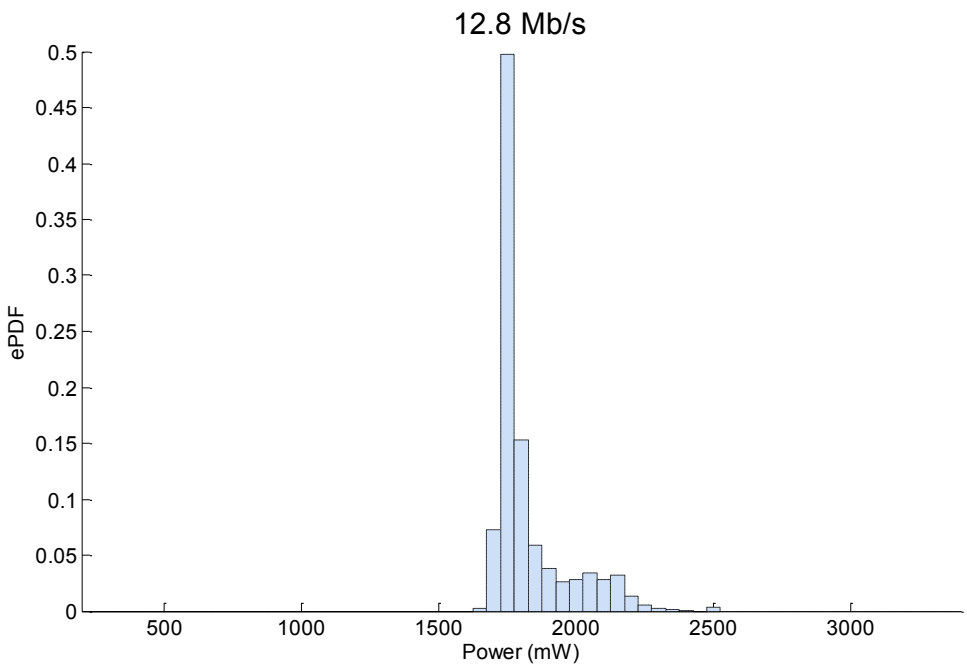

Figure 5.29: Downlink in LTE at 12.8 Mb/s with 90% of quality signal.

5.3.2. Videostreaming.

UMTS.

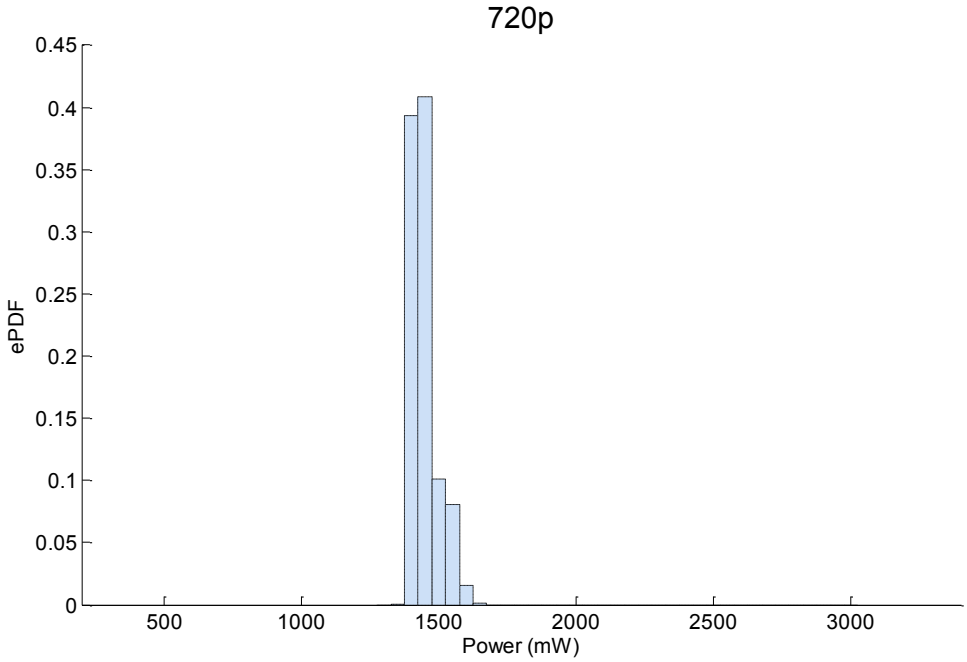

Figure 5.30: Videostreaming in UMTS at a resolution of 720p with 90% of quality signal.

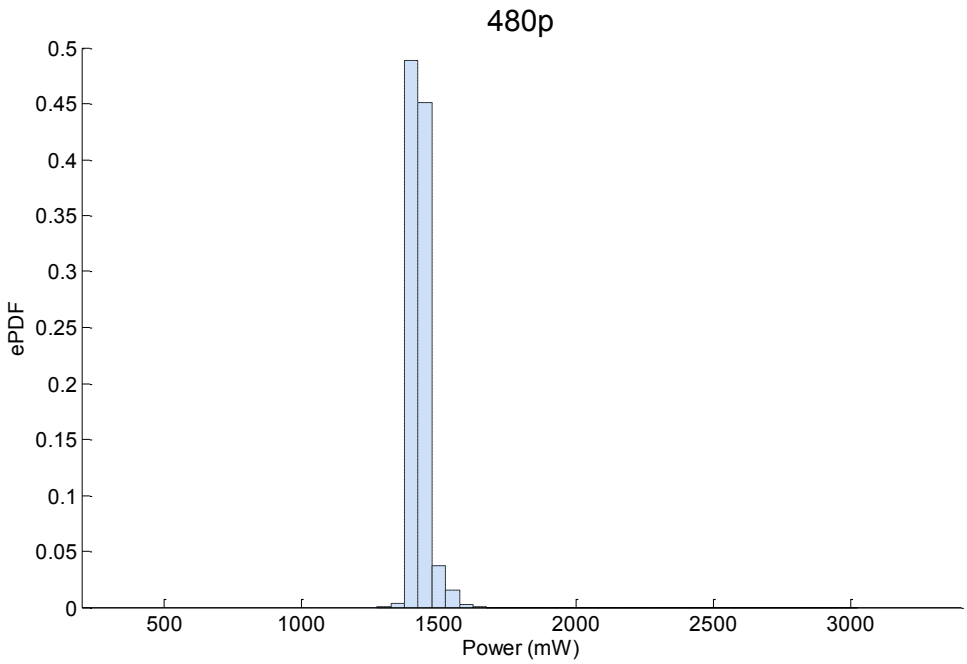

Figure 5.31: Videostreaming in UMTS at a resolution of 480p with 90% of quality signal.

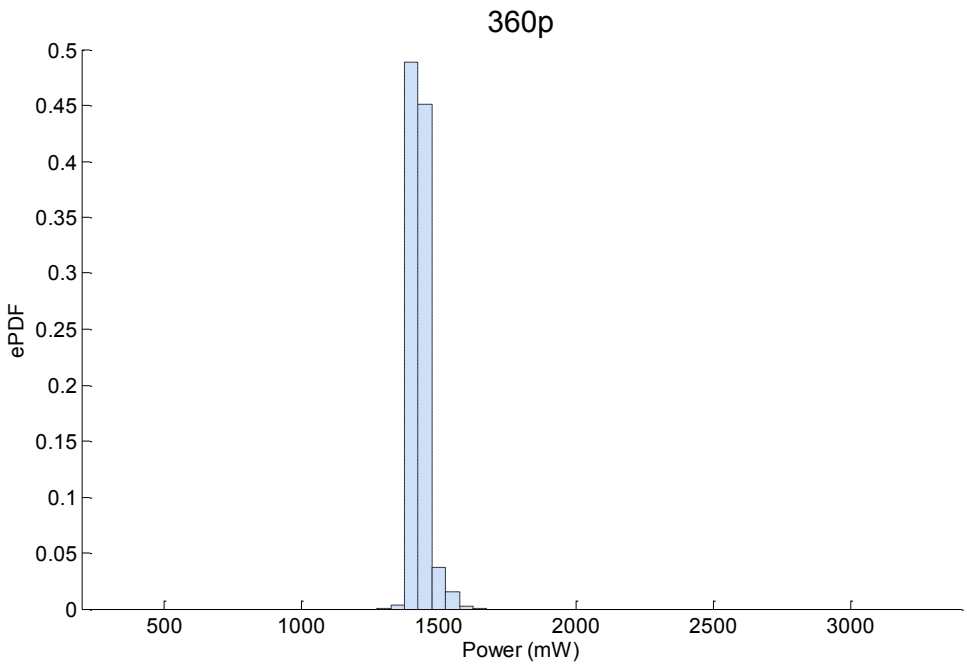

Figure 5.32: Videostreaming in UMTS at a resolution of 360p with 90% of quality signal.

LTE.

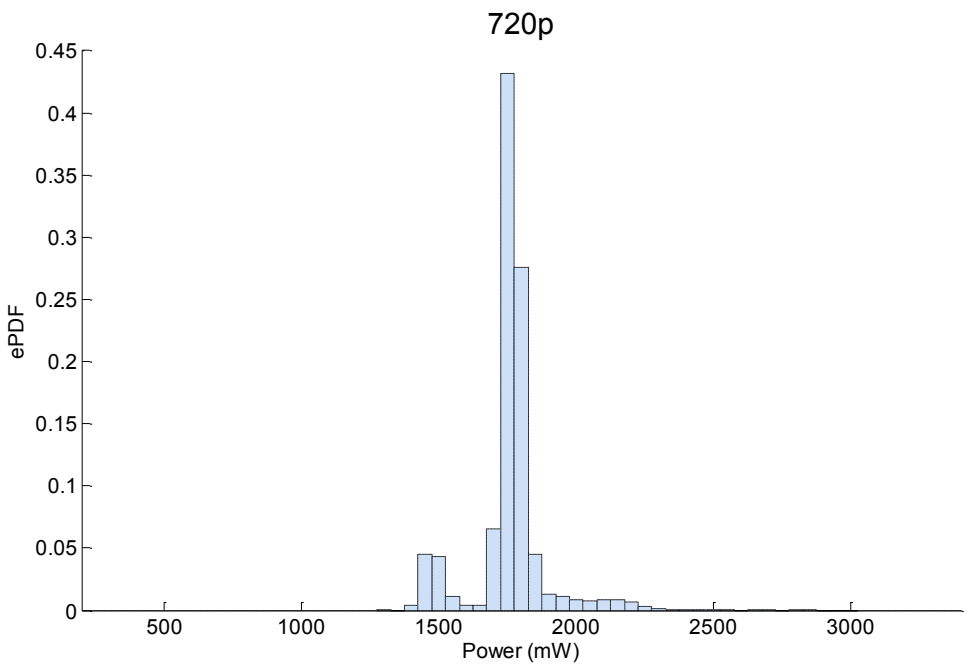

Figure 5.33: Videostreaming in LTE at a resolution of 720p with 90% of quality signal.

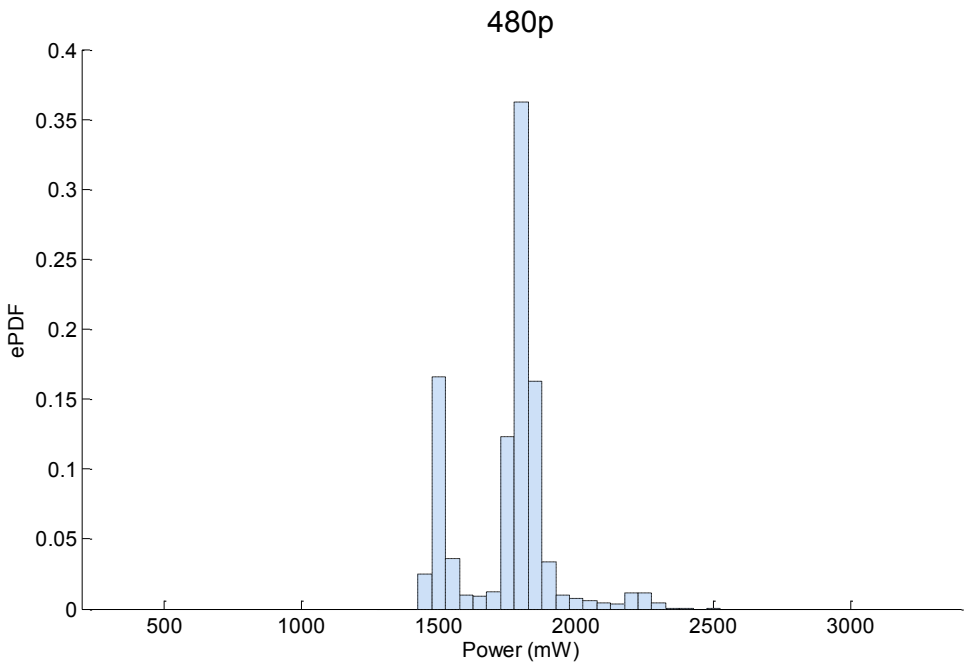

Figure 5.34: Videostreaming in LTE at a resolution of 480p with 90% of quality signal.

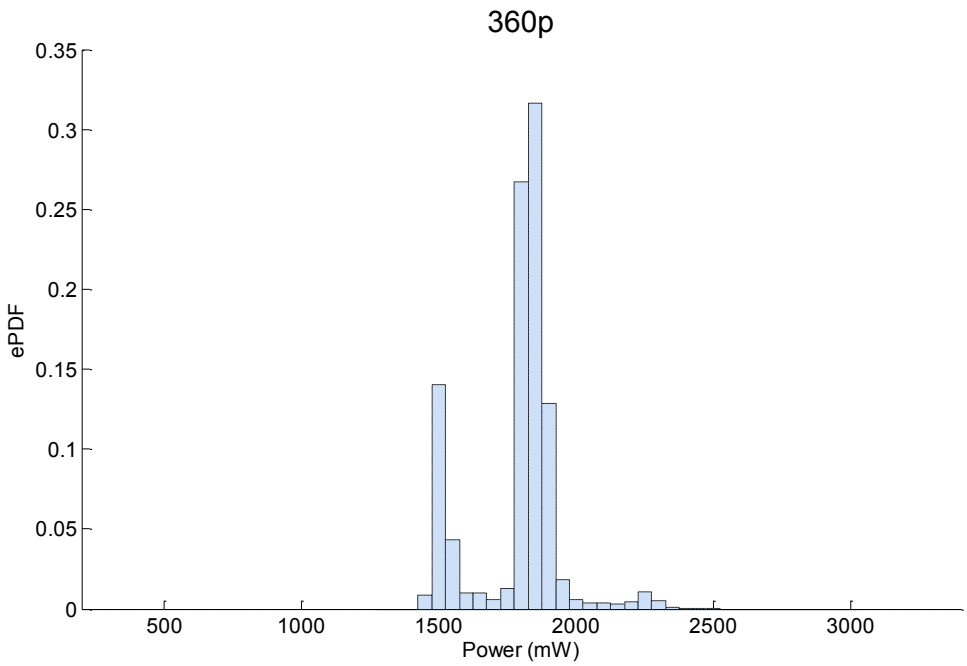

Figure 5.35: Videostreaming in LTE at a resolution of 360p with 90% of quality signal.

5.3.3. Email.

UMTS.

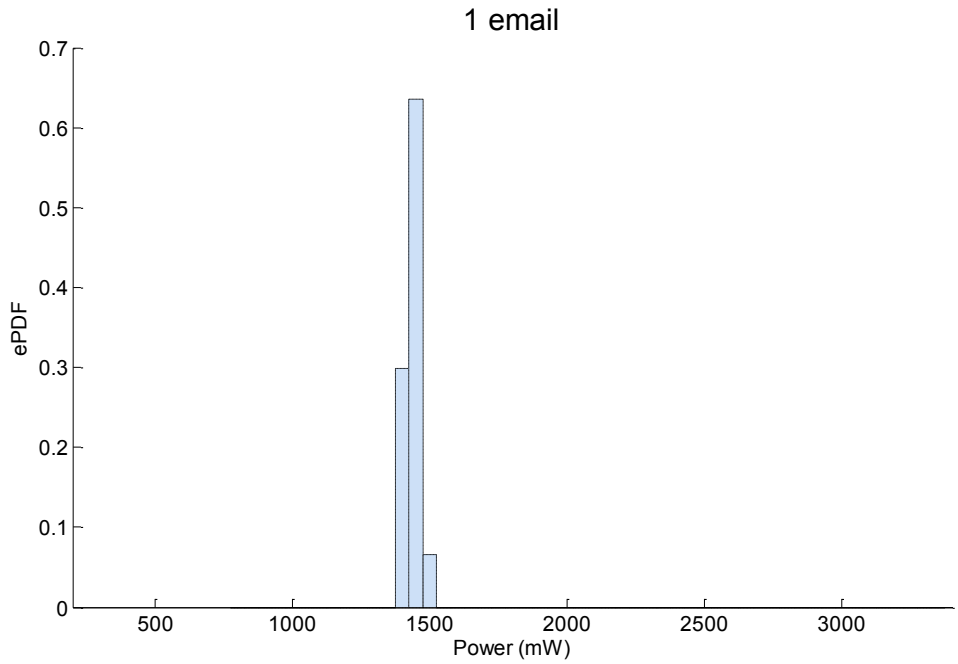

Figure 5.36: Sending in UMTS 1 email with 90% of quality signal.

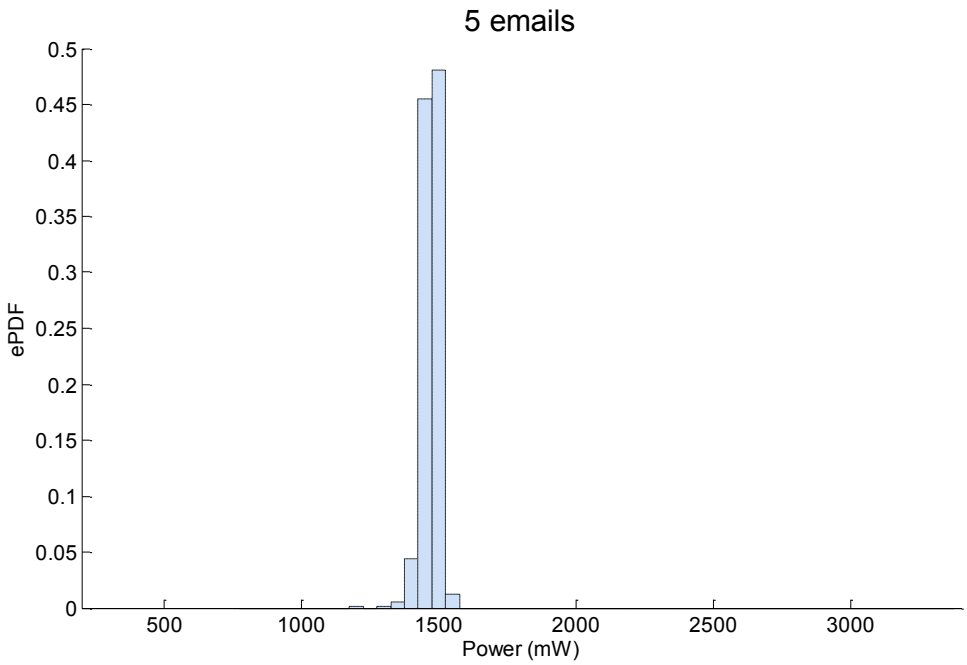

Figure 5.37: Sending in UMTS 5 emails in a row with 90% of quality signal.

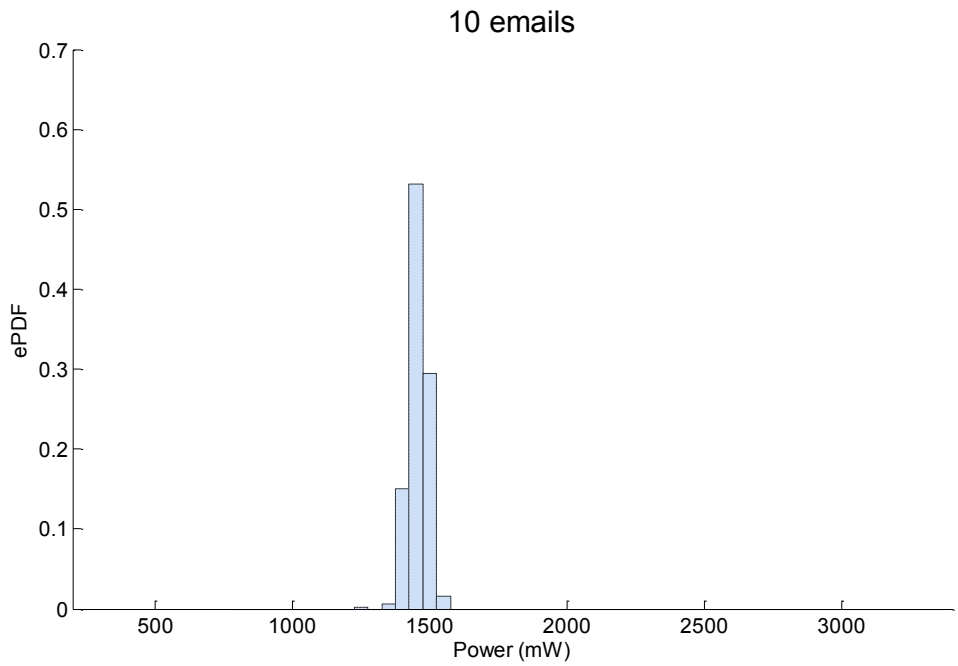

Figure 5.38: Sending in UMTS 10 emails in a row with 90% of quality signal.

LTE.

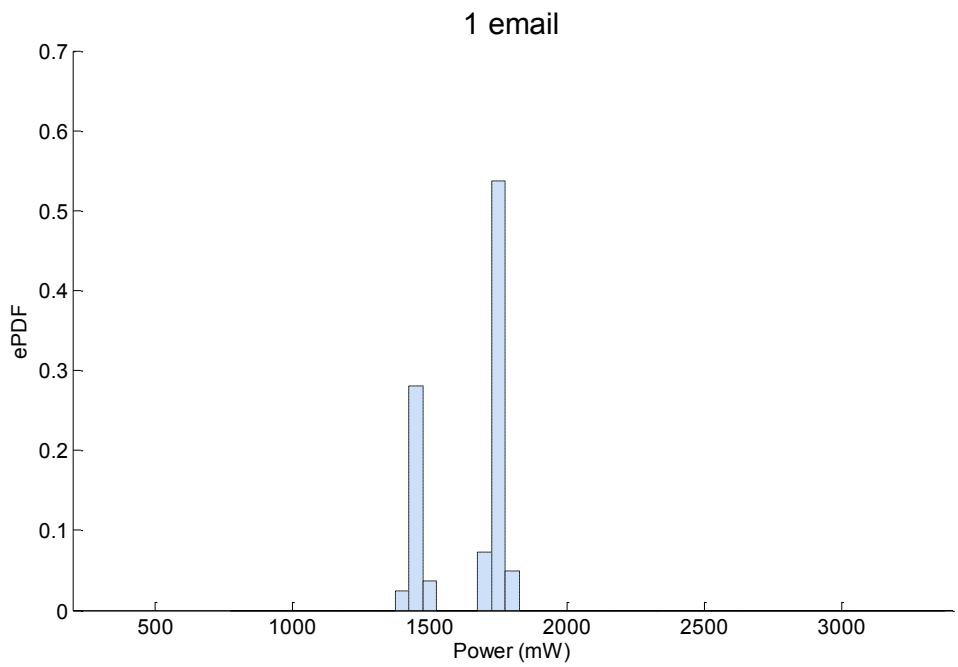

Figure 5.39: Sending in LTE 1 email with 90% of quality signal.

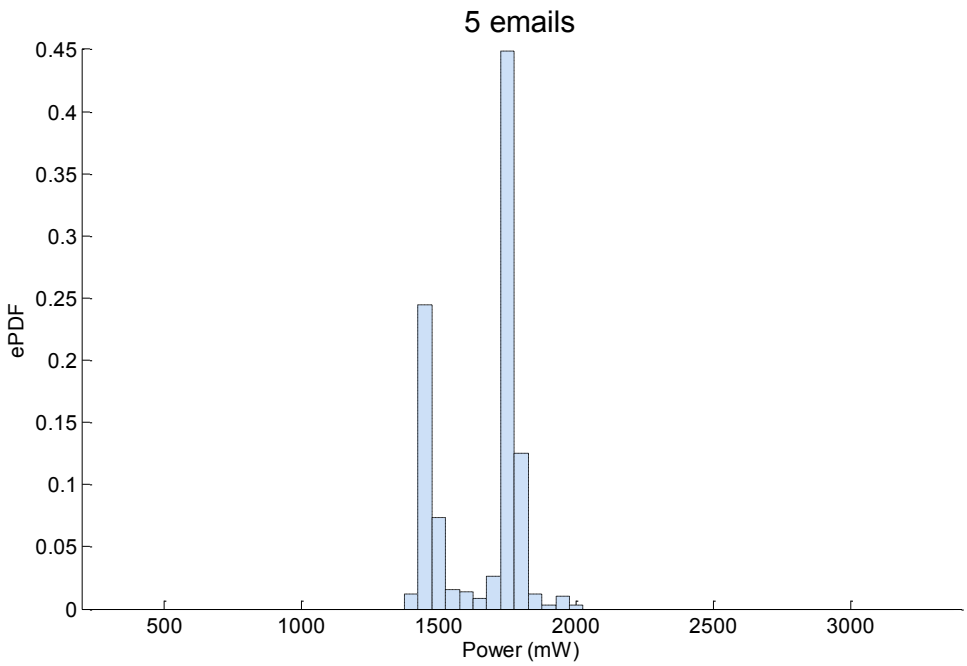

Figure 5.40: Sending in LTE 5 emails in a row with 90% of quality signal.

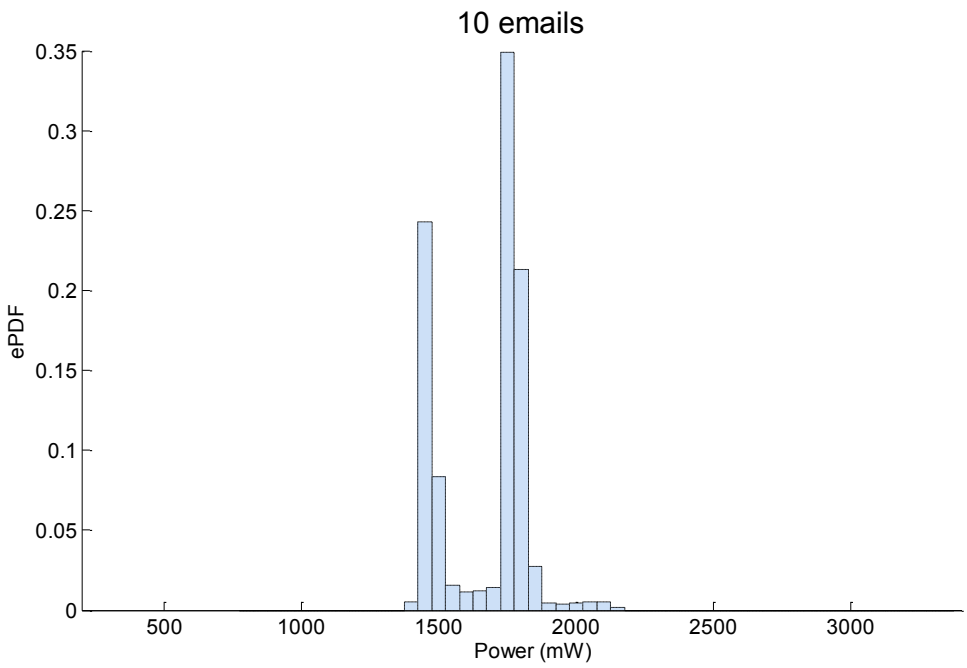

Figure 5.41: Sending in LTE 10 emails in a row with 90% of quality signal.

Chapter 6.

Distribution model.

6.1. Log-normal distribution.

In view of the results obtained, it can be observed that the results show events around discrete states and with higher data rates more time is spent in high power states. Through the software Matlab, it leads to the conclusion that the probability distribution that addapts better to the histograms corresponding to the ePDFs of the power data that have been collected using the implemented software, is the log-normal distribution:

$\mathcal{L}(\mu,\sigma^2)$, where $\sigma > 0$ and $\sigma \in \Re$ is la standard deviation and $\mu \in \Re$ is the mean.

To carry out the modeling of power consumption, in each result the log-normal distribution must be centered in each of the three states and weighted according to the data-rate at the link layer.

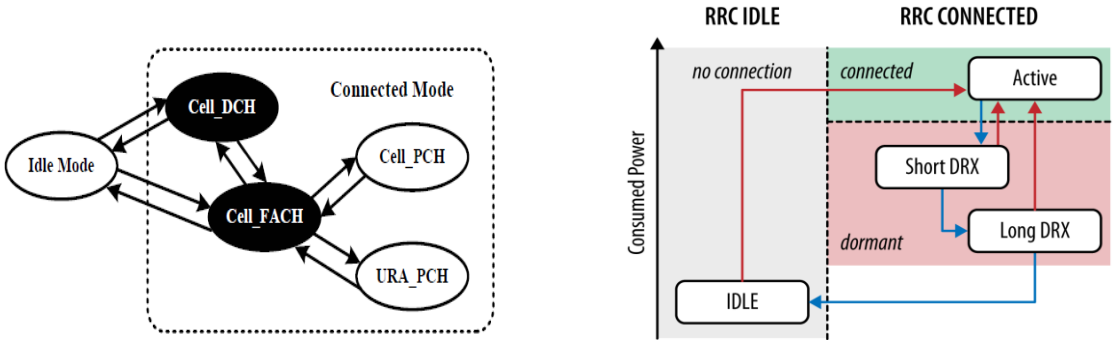

Figure 6.1: RCC state machines for UMTS and LTE.

6.2 Results.

Here are shown some results with the distribution model performed.

Below each graph, it can be seen the results corresponding to the energy consumed measured and the energy consumed modeled. Notice that the error with this approximation is 0.00002 %.

6.2.1. Web traffic.

Uplink.

UMTS.

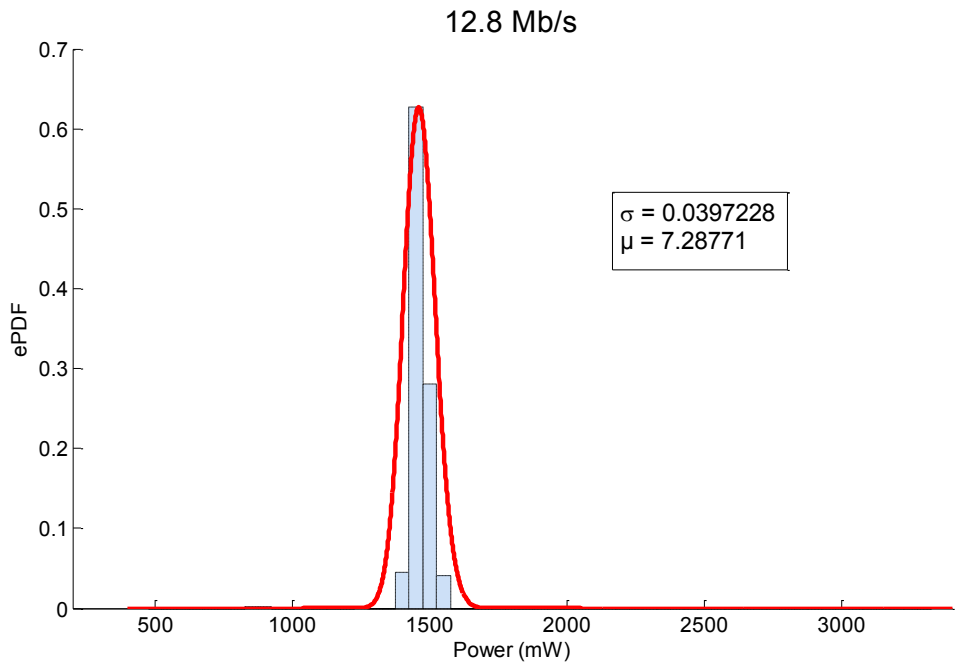

Figure 6.2: Log-normal distribution of uplink in UMTS at 12.8 Mb/s with 55% of quality signal.

Energy consumed measured: 175.7844 J.
Energy consumed modeled: 175.7880 J.

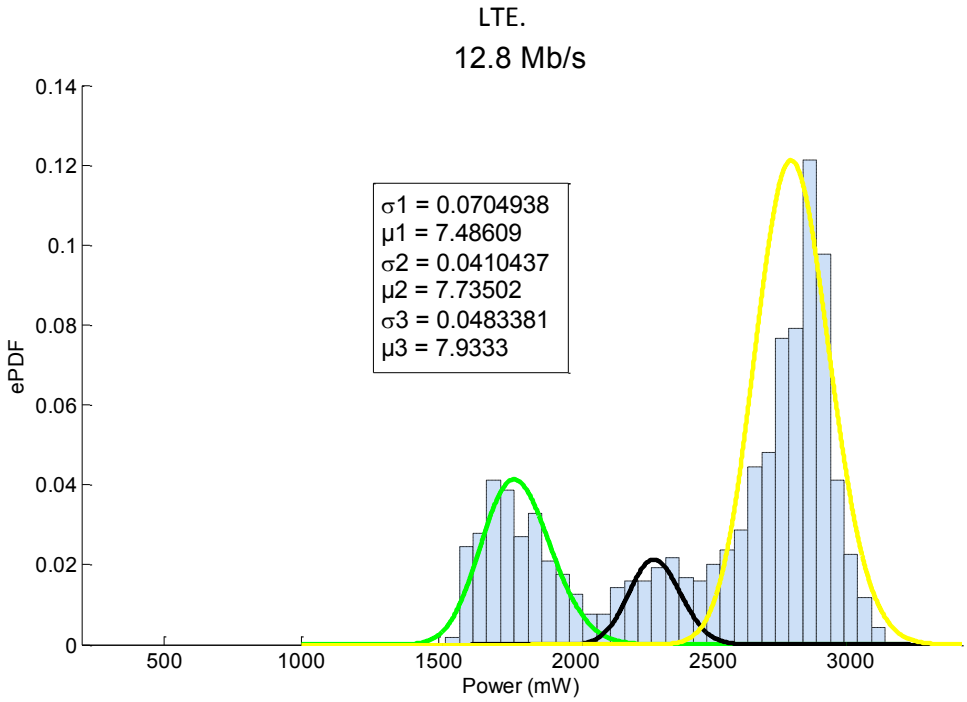

Figure 6.3: Log-normal distribution of uplink in LTE at 12.8 Mb/s with 55% of quality signal.

Energy consumed measured: 3510.1638 J.
Energy consumed modeled: 3510.1620 J.

Here it is noted that in the state of maximum power, the distribution model does not fit quite right. This is because the quality signal is 55%. Although the curve does not fit entirely, it does not affect so much to the final result.

Downlink.

UMTS.

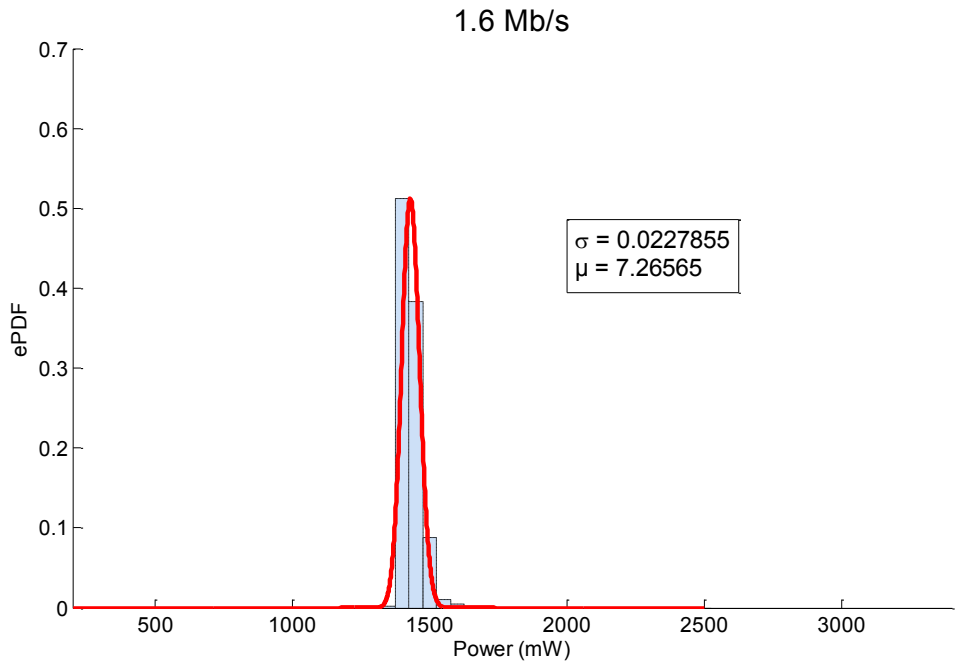

Figure 6.4: Log-normal distribution of uplink in UMTS at 1.6 Mb/s with 90% of quality signal.

Energy consumed measured: 172.7712 J.
Energy consumed modeled: 172.7676 J.

LTE.

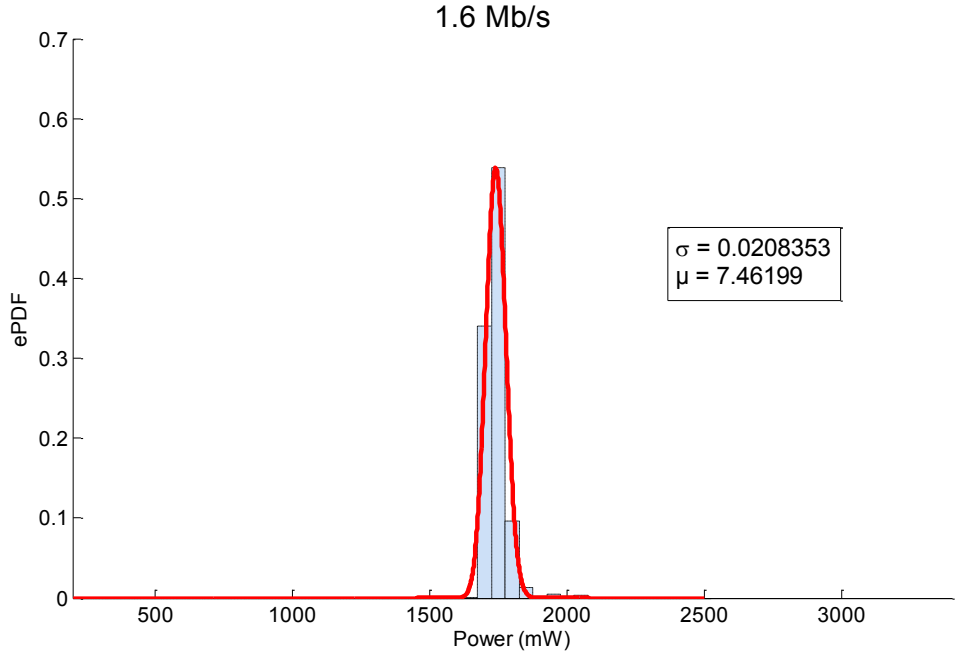

Figure 6.5: Log-normal distribution of uplink in LTE at 1.6 Mb/s with 90% of quality signal.

Energy consumed measured: 211.7088 J.
Energy consumed modeled: 211.7091 J.

6.2.2. Video.

UMTS.

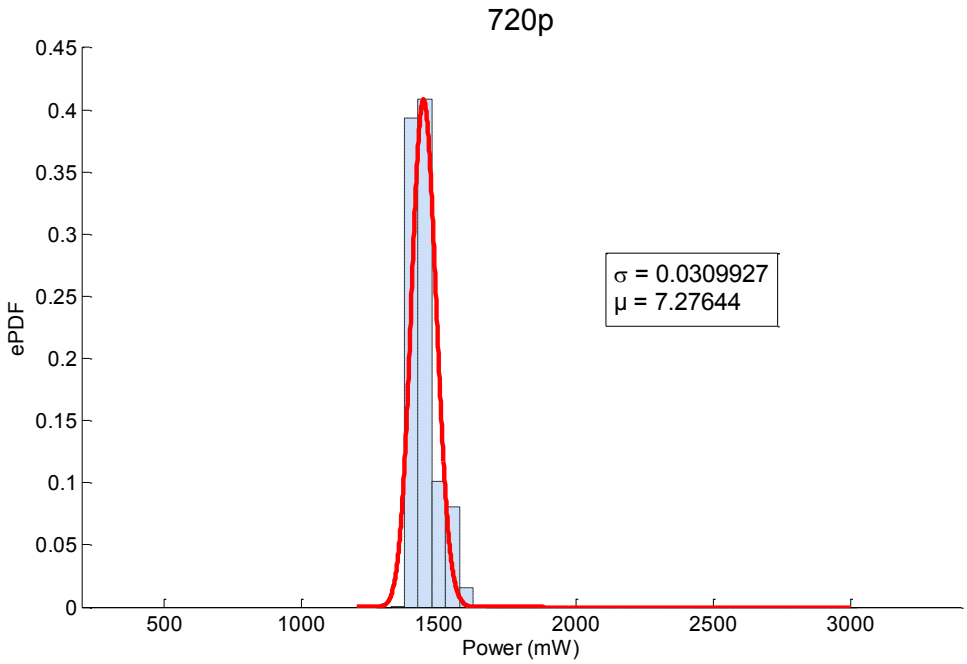

Figure 6.6: Log-normal distribution of a videostreaming in UMTS at a resolution of 720p with 90% of quality signal.

Energy consumed measured: 2604.9996 J.
Energy consumed modeled: 2604.9960 J.

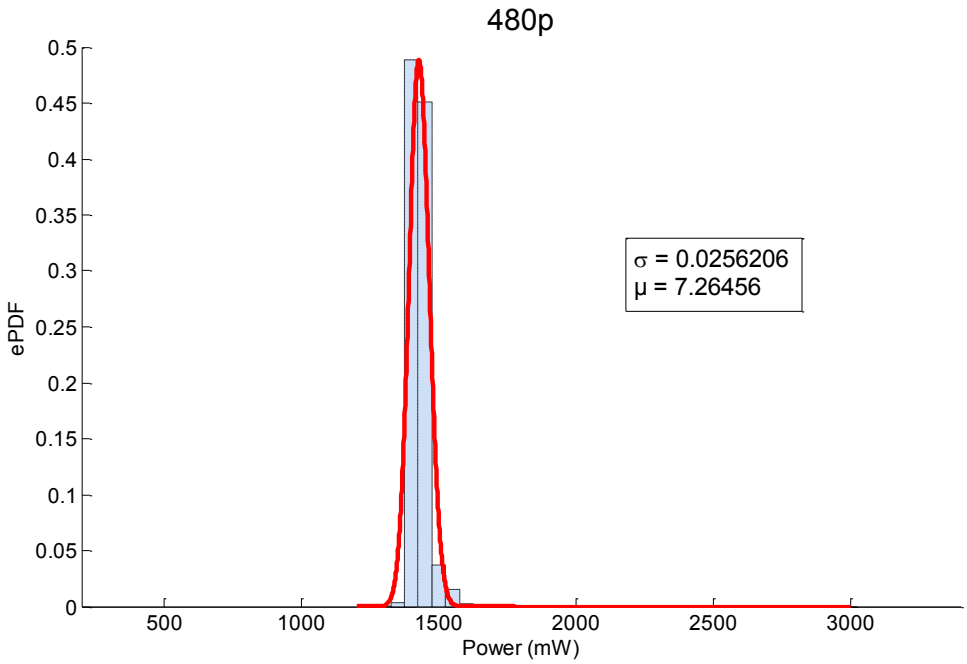

Figure 6.7: Log-normal distribution of a videostreaming in UMTS at a resolution of 480p with 90% of quality signal.

Energy consumed measured: 2572.9128 J.
Energy consumed modeled: 2572.9092 J.

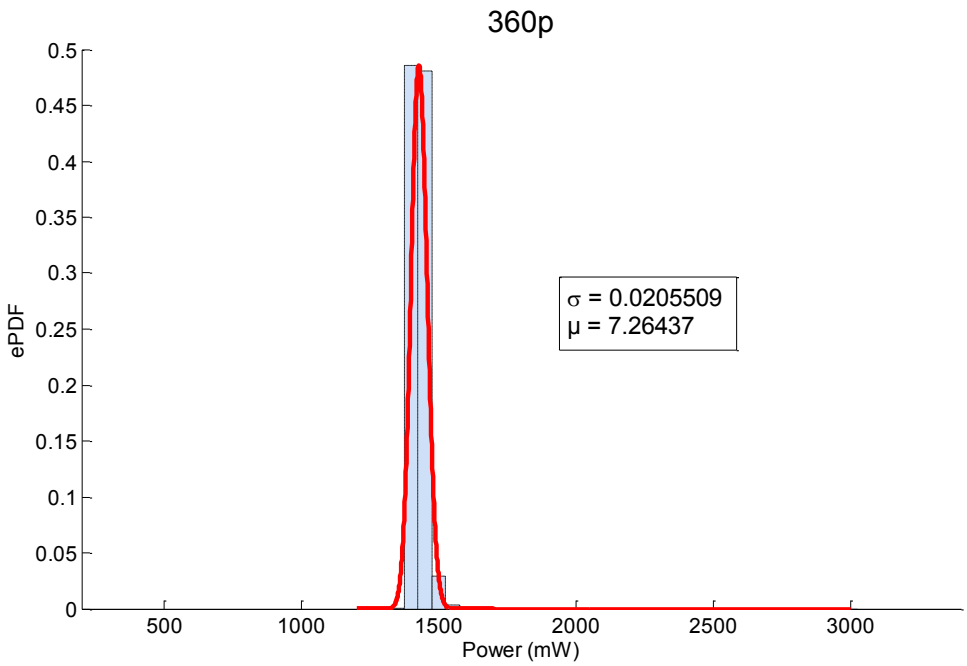

Figure 6.8: Log-normal distribution of a videostreaming in UMTS at a resolution of 360p with 90% of quality signal.

Energy consumed measured: 2571.9516 J.
Energy consumed modeled: 2571.9480 J.

LTE.

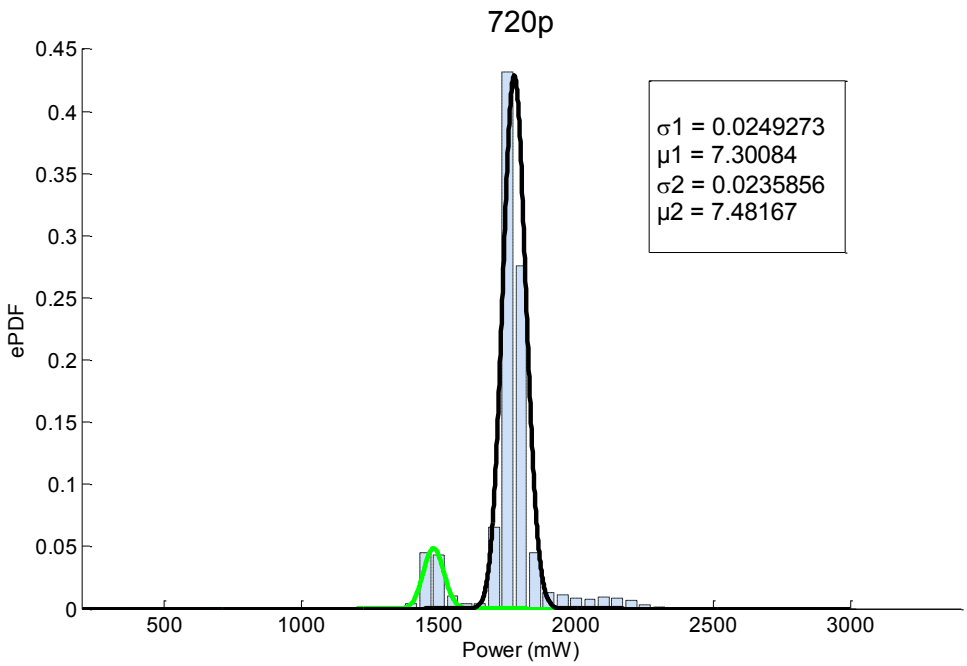

Figure 6.9: Log-normal distribution of a videostreaming in LTE at a resolution of 720p with 90% of quality signal.

Energy consumed measured: 3163.0680 J.
Energy consumed modeled: 3163.0716 J.

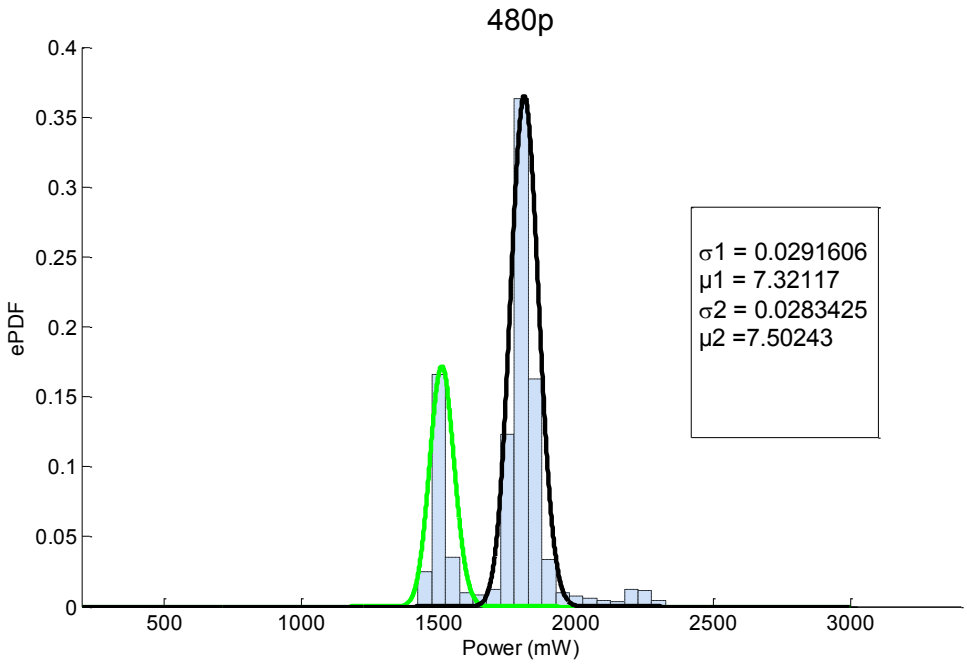

Figure 6.10: Log-normal distribution of a videostreaming in LTE at a resolution of 480p with 90% of quality signal.

Energy consumed measured: 3154.0824 J.
Energy consumed modeled: 3154.0788 J.

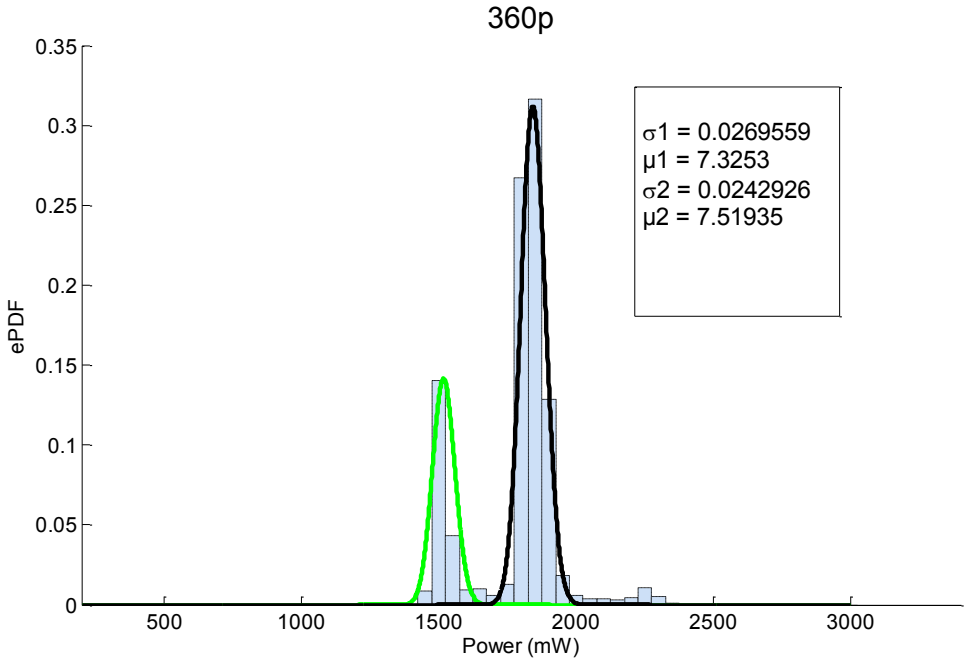

Figure 6.11: Log-normal distribution of a videostreaming in LTE at a resolution of 360p with 90% of quality signal.

Energy consumed measured: 3135.0096 J.
Energy consumed modeled: 3135.0132 J.

6.2.3. Emails sending.

UMTS.

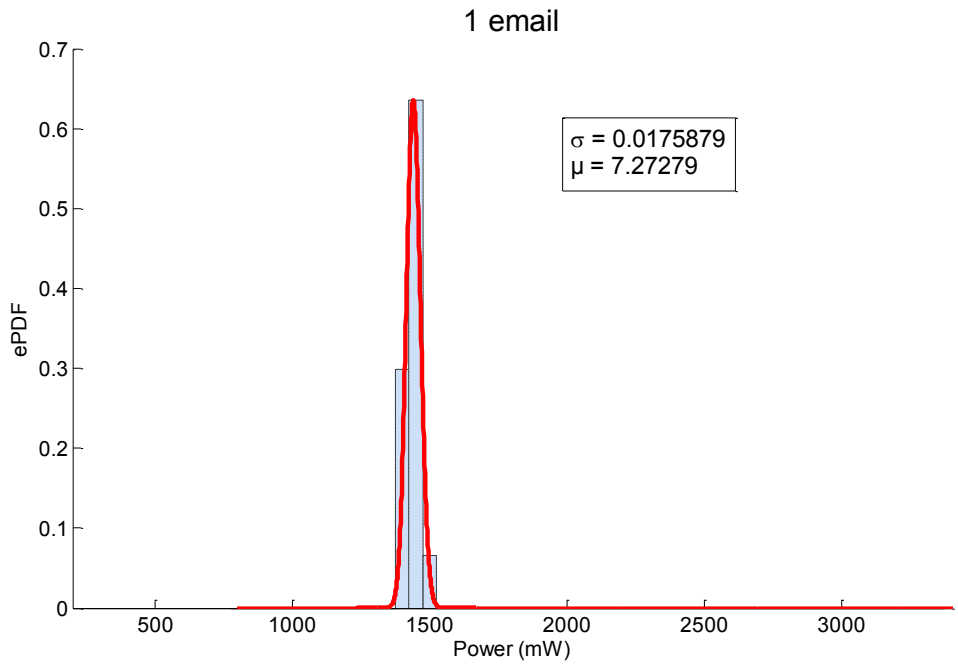

Figure 6.12: Log-normal distribution of sending 1 email in LTE with 90% of quality signal.

Energy consumed measured: 16.9473 J.
Energy consumed modeled: 16.9466 J.

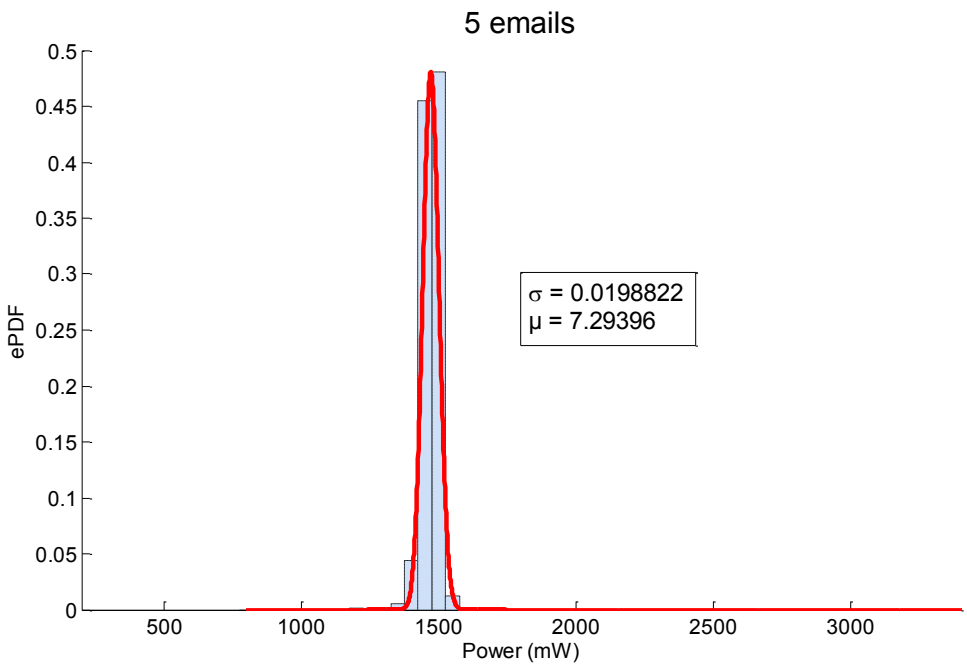

Figure 6.13: Log-normal distribution of sending 5 emails in a row in UMTS with 90% of quality signal.

Energy consumed measured: 89.6328 J.
Energy consumed modeled: 89.6292 J.

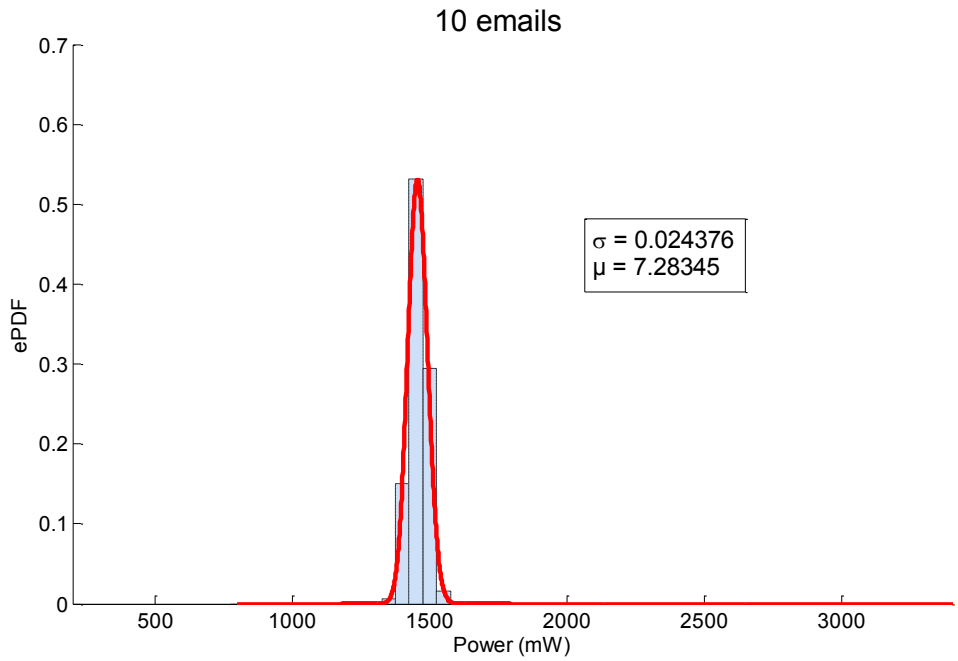

Figure 6.14: Log-normal distribution of sending 10 emails in a row in UMTS with 90% of quality signal.

Energy consumed measured: 174.1017 J.
Energy consumed modeled: 174.1020 J.

LTE.

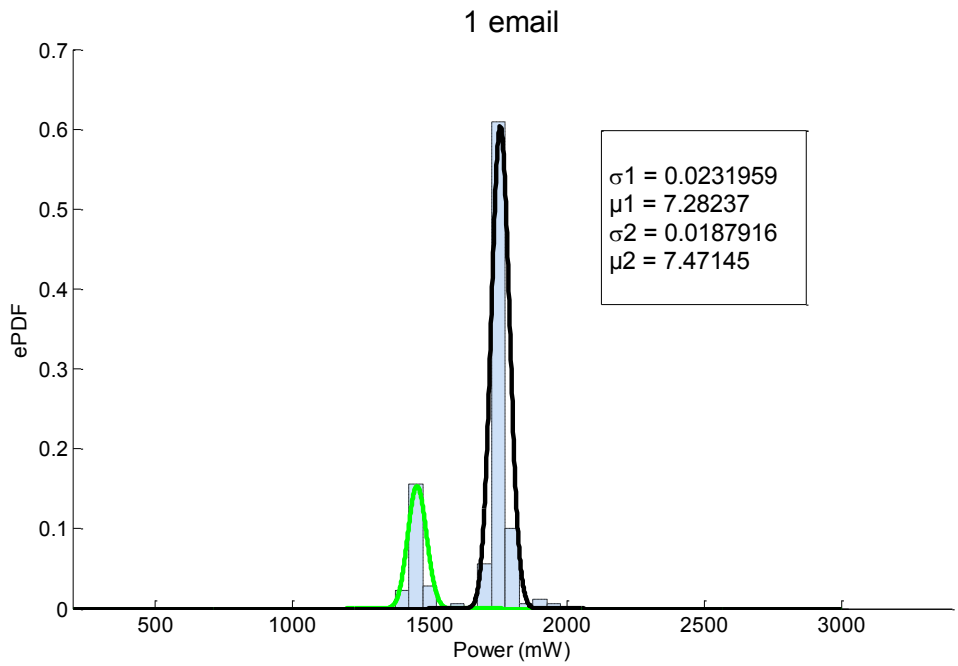

Figure 6.15: Log-normal distribution of sending 1 email in LTE with 90% of quality signal.

Energy consumed measured: 30.3087 J.
Energy consumed modeled: 30.3084 J.

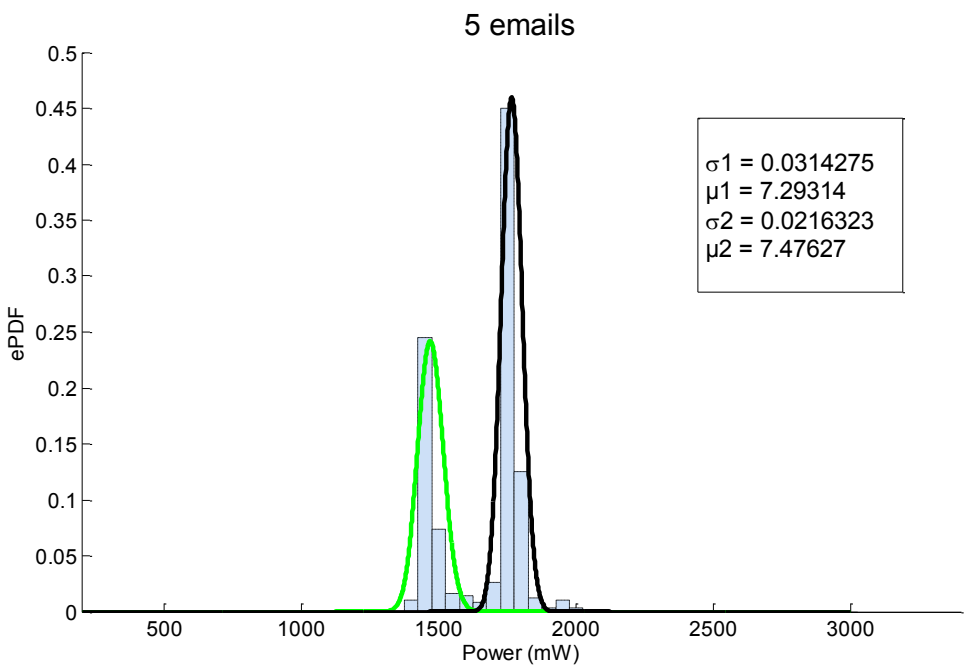

Figure 6.16: Log-normal distribution of sending 5 emails in a row in LTE with 90% of quality signal.

Energy consumed measured: 93.9589 J.
Energy consumed modeled: 93.9598 J.

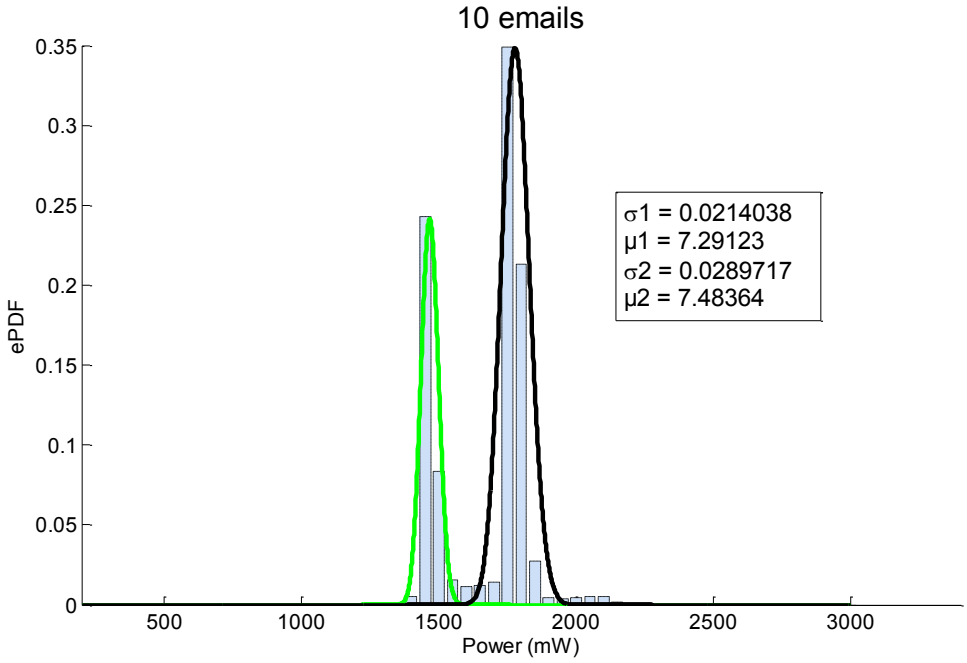

Figure 6.17: Log-normal distribution of sending 10 emails in a row in LTE with 90% of quality signal.

Energy consumed measured: 189.3076 J.
Energy consumed modeled: 189.3078 J.

Chapter 7.

Conclusions and outlook.

Throughout this Master Thesis, a Power Meter setup for USB has been carried out. A software base recording was implemented to record hundreds of traces over email, streaming and web traffic, this one using a software based traffic pattern generator. The impact on supply power for UMTS and LTE was studied, first depending only on traffic pattern and then depending on signal quality too. Finally a model for estimating power consumption was found, using the log-normal distribution. In this model, it is noted that the μ parameter, corresponding to the mean, it increases as the data rate increases because the higher the data rate, the more time is spent in high power states, so it needs more energy.

It has been observed, in the section of web traffic, that more energy is needed for Uplink than for Downlink, due to the company of the SIM card (A1 Telekom Austria) uses higher frequencies for Uplink than for Downlink what imply more energy.

Another conclusion is that it is also needed more energy when the quality signal falls, due to the packet loss. So a component of uploading appears when some packets have not arrived and the protocol has to request them again.

In all the results obtained, if both technologies (UMTS and LTE) are compared, it can be noticed that with LTE the modem consumes more energy. This is because, as seen in section 3.2.4, LTE causes a larger energy drain for the same amount of content due to the high power used in the Long DRX tail state.

In the results that there are three states, when the quality reception is 55%, the curve of the maximum power state does not fit quite right, but then the result itself is quite good. A future work could be fitting better this curve.

Current model works only for the measured radio conditions, so another future work could be seeing if it also works for different radio conditions.

Finally, since the software has been implemented for the operative system Windows, it could be implemented for other operative systems.

Appendix A.

USB Power Meter features.

- Atmega 32u4 (all unused pins are broken out).
- INA219B Current IC from TI.
- INA219B can measure up to 3.6Amps in its current configuration (adjustable in library code).
- LED Threshold Warning indicator (configurable via desktop application).
- Can be powered from the same source as the measuring device or from a separate USB port, it does not affect the measurements.
- Header connection to OLED display.
- Arduino Leonardo bootloader for easy hacking.
- Source code available for download.

Adafruit OLED Display:

- 128×32 pixel monochrome OLED Display.
- SPI Interface to Microcontroller.
- Daylight readable.
- Low power with OLED technology.
- Able to display graphics and characters.

Appendix B.

USB modem features.

B.1. Main features.

The E392 mainly supports the following features:

- LTE 2600MHz/2100MHz/1800MHz/900MHz/DD800MHz, DC-HSPA+/HSPA+/UMTS 2100MHz/1800MHz/900MHz, GSM/GPRS/EDGE. 850MHz/900MHz/1800MHz/1900MHz.
- Support LTE 2600 10M/20M bandwidth.
- Support LTE 2100 5M/10M bandwidth.
- Support LTE 1800 15M/20M bandwidth.
- Support LTE 900 5M/10M bandwidth.
- Support LTE DD800 5M/10M bandwidth.
- LTE 2×2 MIMO.
- LTE uplink data service of up to 50Mbps.
- LTE downlink data service of up to 100Mbps.
- HSPA+ data service of up to 42Mbps (Dual carrier).
- HSDPA/HSPA+ Equalizer and receive diversity (TYPE 3).
- HSPA+ data service of up to 21Mbps (64QAM).
- HSUPA data service of up to 5.76Mbps.
- HSDPA data service of up to 14.4Mbps.
- UMTS PS domain data service of up to 384 kbps.
- EDGE packet data service of up to 296kbps on DL with MSC33.
- GPRS packet data service of up to 85.6 kbps.
- CS domain data service based on UMTS and GSM.
- SMS based on CS/PS domain of GSM and WCDMA.
- WCDMA/GSM SMS service.
- Prepared for LTE SMS over SGs service, but not activated.
- Support LTE intra-frequency handover, inter-frequency handover will be supported by firmware upgrade later.
- Support LTE and UMTS inter-RAT idle mobility, LTE and GERAN inter-RAT idle mobility will be supported by firmware upgrade later.
- Inter-RAT connected mobility will be supported by firmware upgrade later.
- Automatic installation.
- Standard USB interface (Type A).
- Micro SD card Slot.

- External antenna interface.
- Windows XP SP2/SP3, Windows Vista SP1/SP2, Windows 7, Mac OS X 10.5, 10.6 with latest upgrades.

B.2. System architecture.

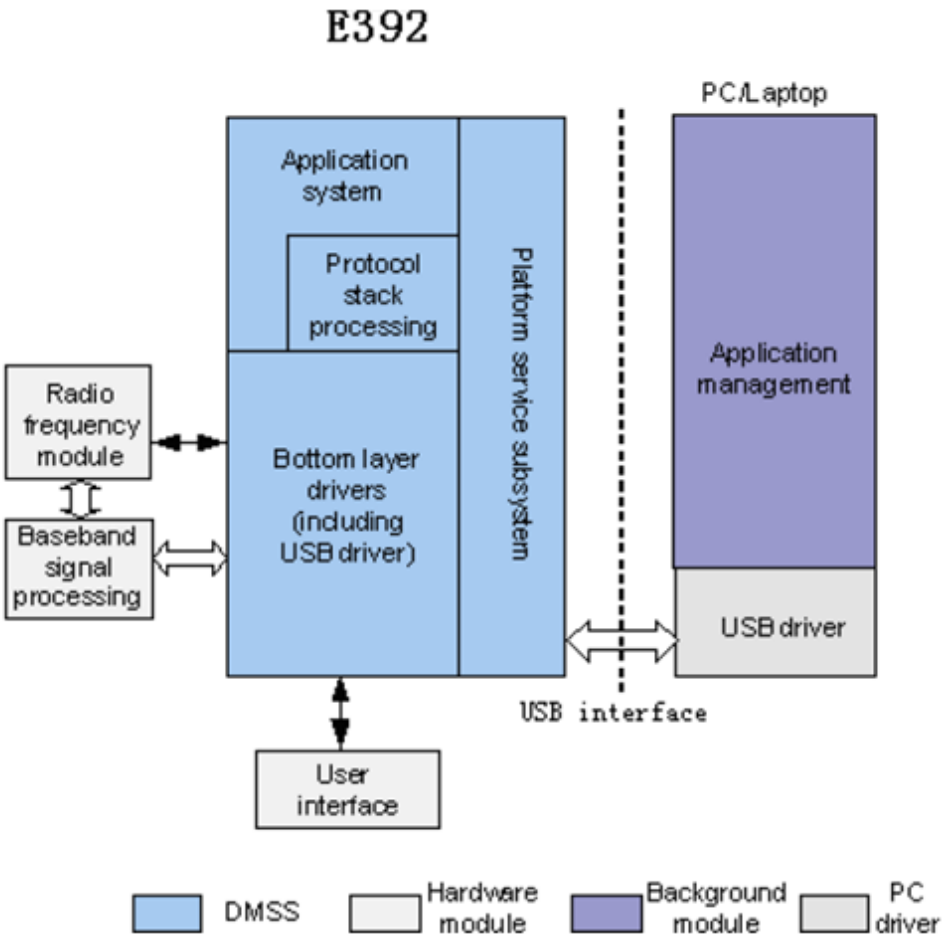

Figure B.1: Scheme of the system architecture of the USB modem.

Appendix C.

Web traffic results.

C.1. Measurements with 55% of signal quality.

C.1.1. Uplink.

UMTS.

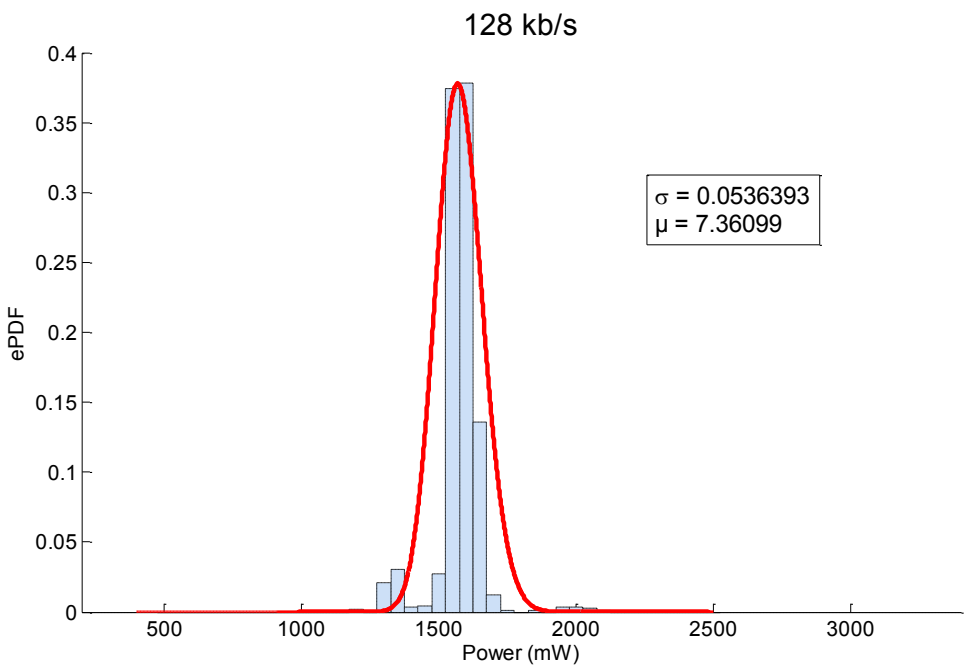

Figure C.1: Log-normal distribution of uplink in UMTS at 128 kb/s with 55% of quality signal.

Energy consumed measured: 190.4904 J.
Energy consumed modeled: 190.4940 J.

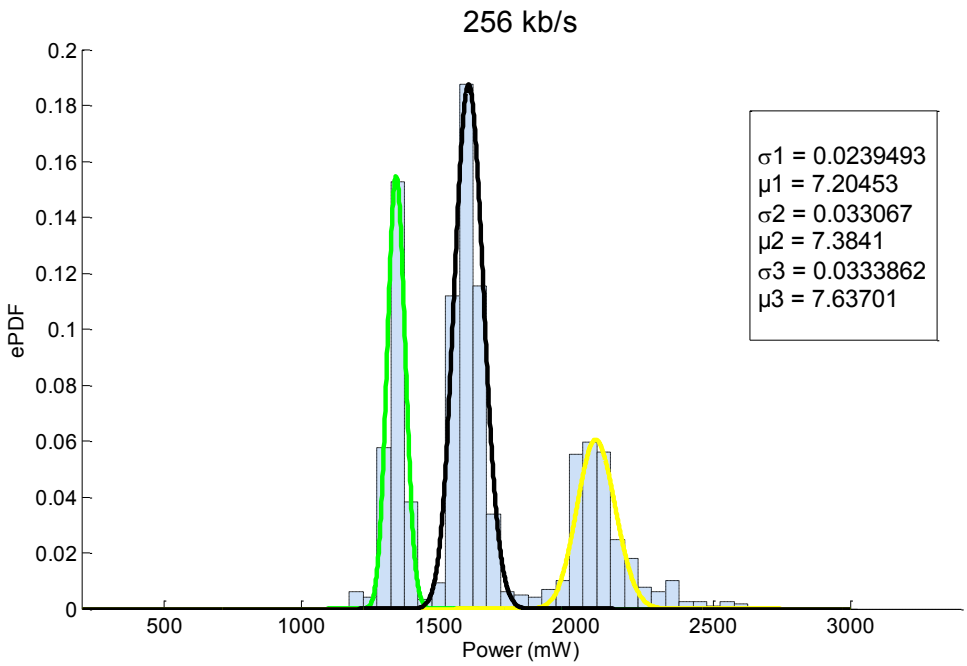

Figure C.2: Log-normal distribution of uplink in UMTS at 256 kb/s with 55% of quality signal.

Energy consumed measured: 190.4904 J.
Energy consumed modeled: 190.4968 J.

LTE.

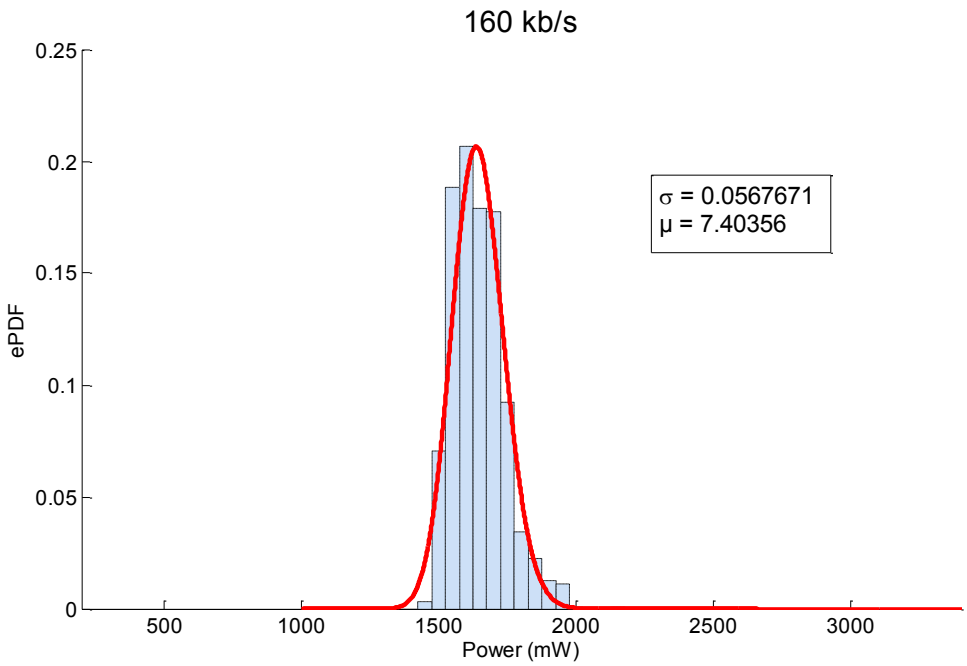

Figure C.3: Log-normal distribution of uplink in LTE at 160 kb/s with 55% of quality signal.

Energy consumed measured: 196.6248 J.
Energy consumed modeled: 196.6284 J.

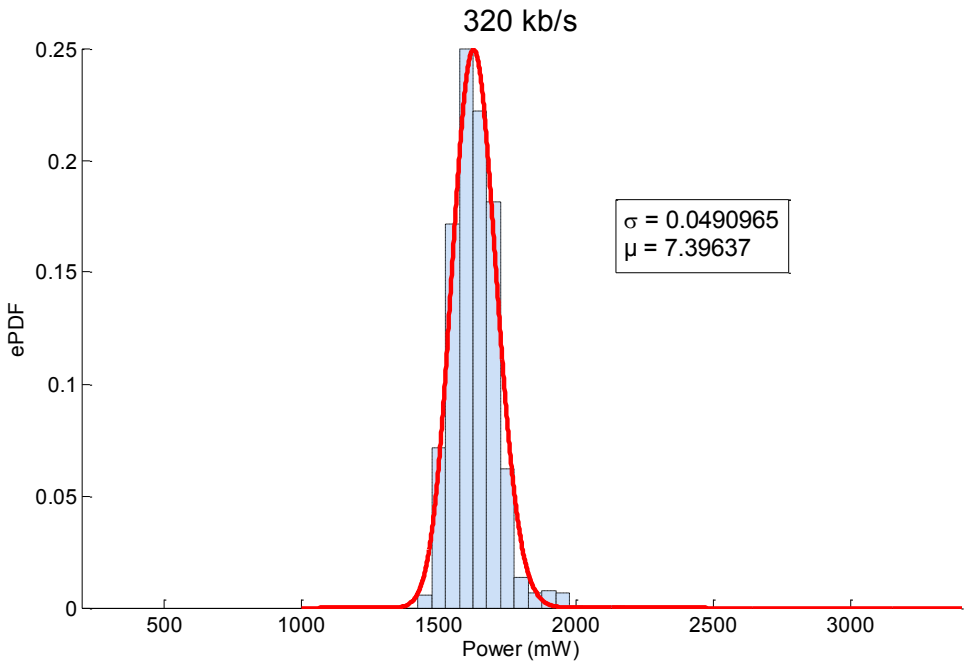

Figure C.4: Log-normal distribution of uplink in LTE at 320 kb/s with 55% of quality signal.

Energy consumed measured: 198.0756 J.
Energy consumed modeled: 198.0720 J.

C.1.2. Downlink.

UMTS.

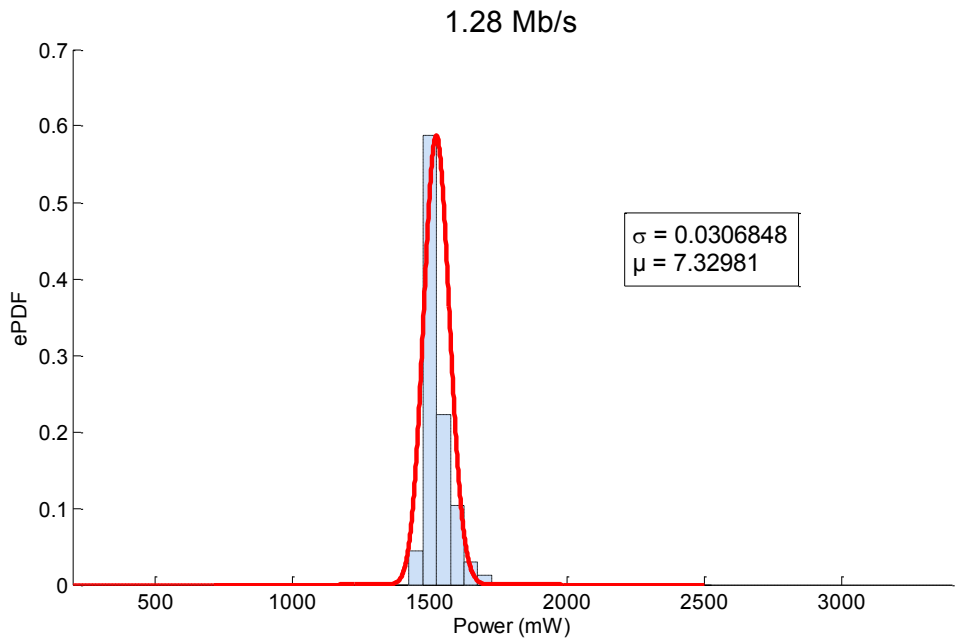

Figure C.5: Log-normal distribution of downlink in UMTS at 1.28 Mb/s with 55% of quality signal.

Energy consumed measured: 184.0860 J.
Energy consumed modeled: 184.0896 J.

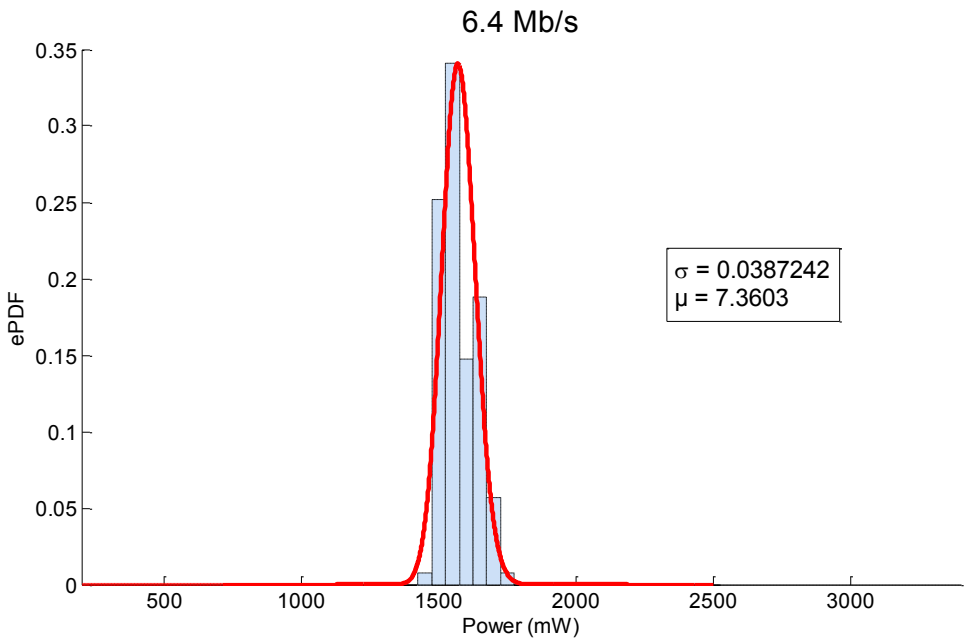

Figure C.6: Log-normal distribution of downlink in UMTS at 6.4 Mb/s with 55% of quality signal.

Energy consumed measured: 188.9640 J.
Energy consumed modeled: 188.9676 J.

LTE.

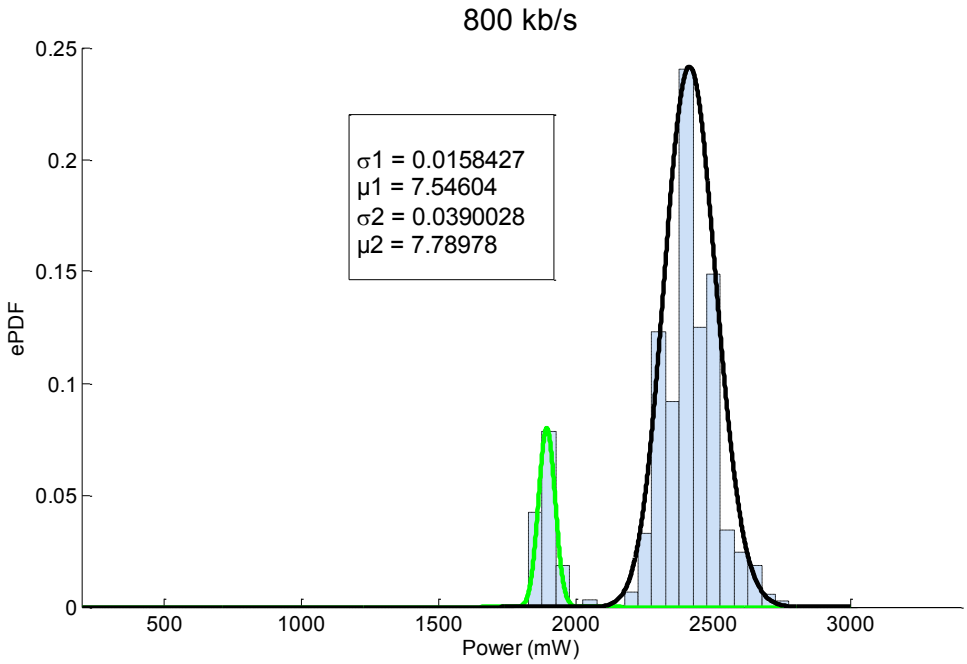

Figure C.7: Log-normal distribution of downlink in LTE at 800 kb/s with 55% of quality signal.

Energy consumed measured: 283.4064 J.
Energy consumed modeled: 283.4100 J.

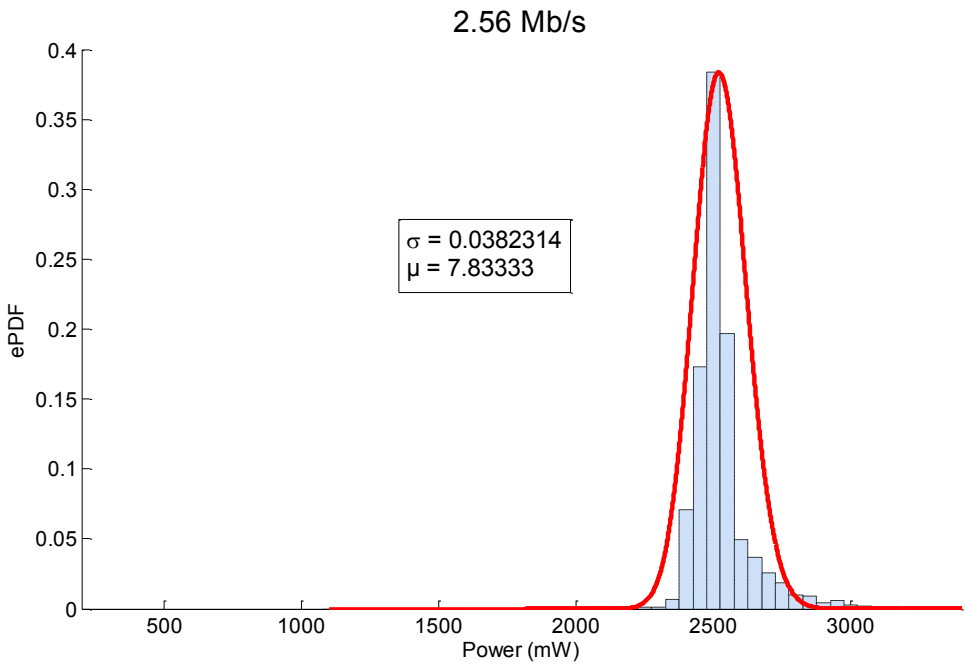

Figure C.8: Log-normal distribution of downlink in LTE at 2.56 Mb/s with 55% of quality signal.

Energy consumed measured: 303.9372 J.
Energy consumed modeled: 303.9408 J.

C.2. 90% of quality signal.

C.2.1. Uplink.

UMTS.

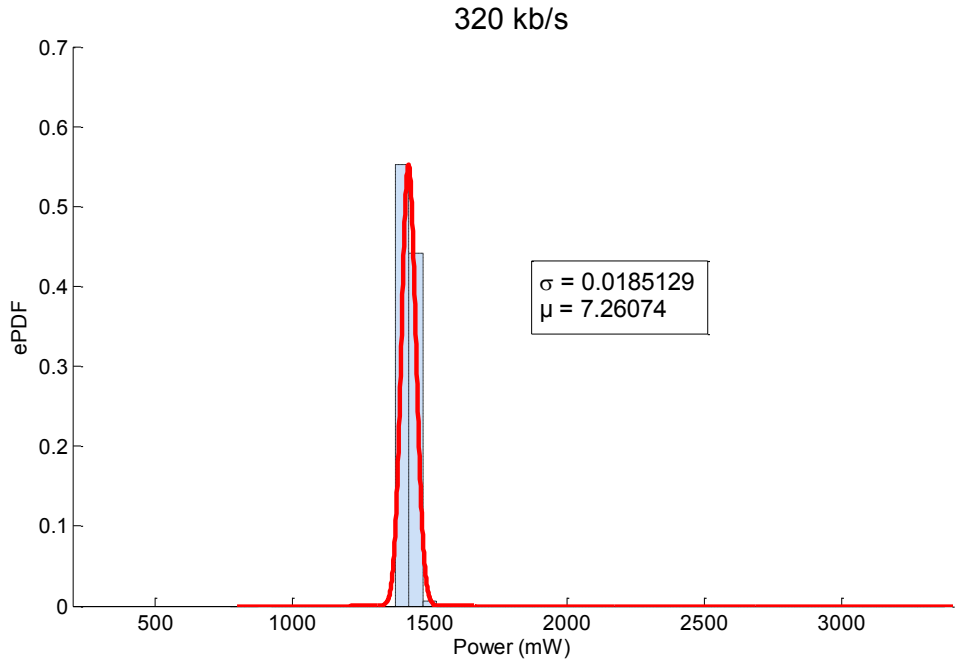

Figure C.9: Log-normal distribution of uplink in UMTS at 320 kb/s with 90% of quality signal.

Energy consumed measured: 170.8488 J.
Energy consumed modeled: 170.8452 J.

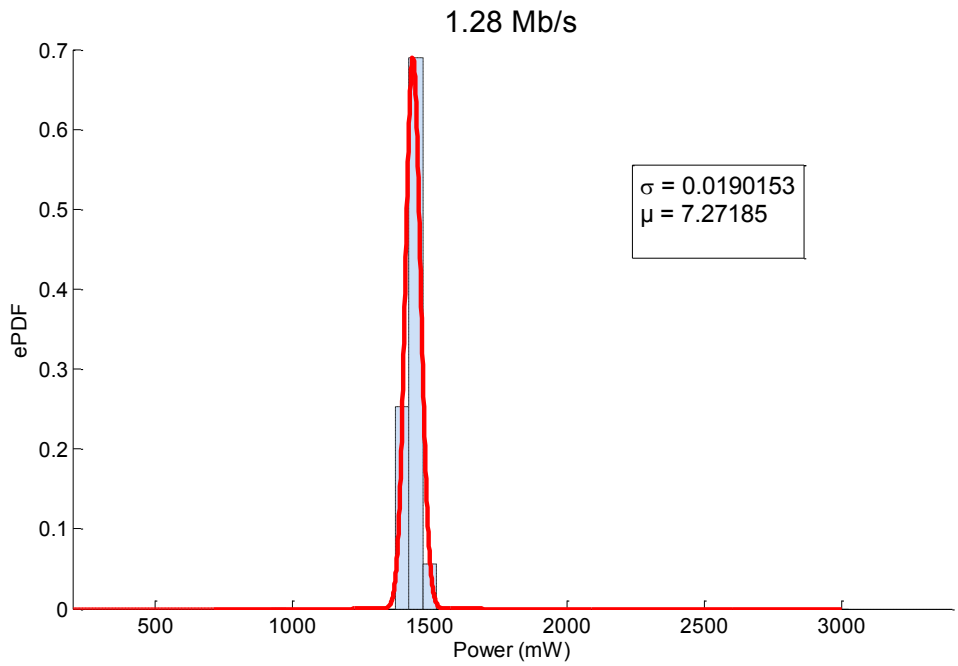

Figure C.10: Log-normal distribution of uplink in UMTS at 1.28 Mb/s with 90% of quality signal.

Energy consumed measured: 171.7776 J.
Energy consumed modeled: 171.7812 J.

LTE.

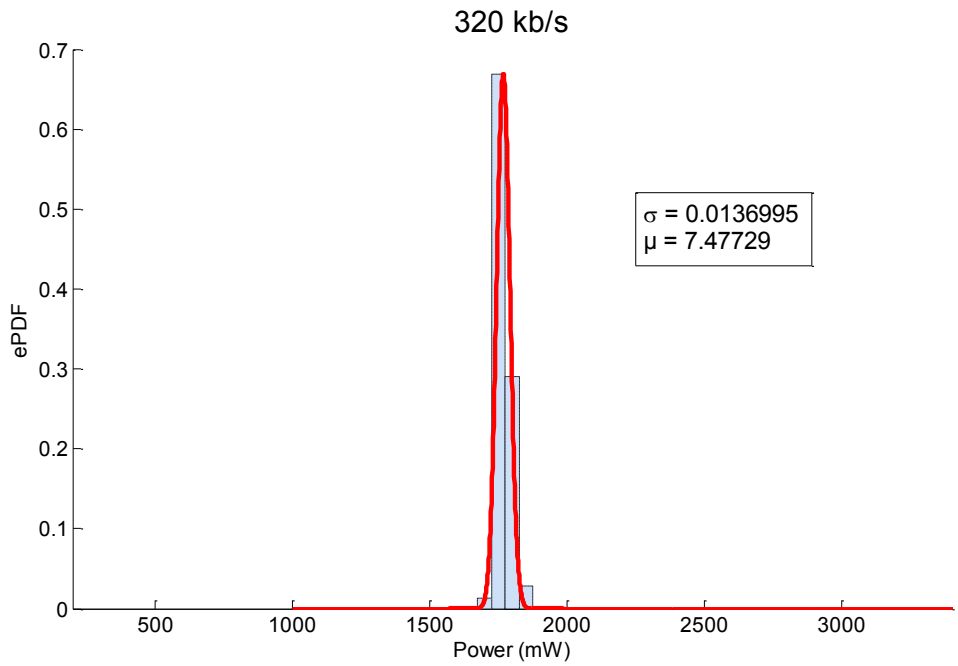

Figure C.11: Log-normal distribution of uplink in LTE at 320 kb/s with 90% of quality signal.

Energy consumed measured: 212.2992 J.
Energy consumed modeled: 212.3028 J.

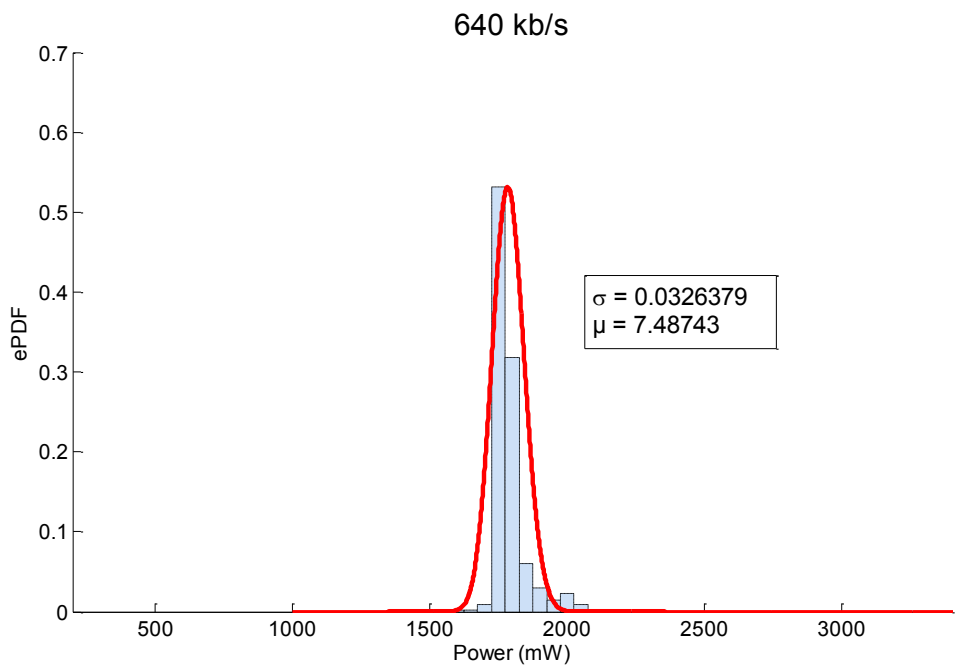

Figure C.12: Log-normal distribution of uplink in LTE at 640 kb/s with 90% of quality signal.

Energy consumed measured: 764.2901 J.
Energy consumed modeled: 764.2904 J.

C.2.2. Downlink.

UMTS.

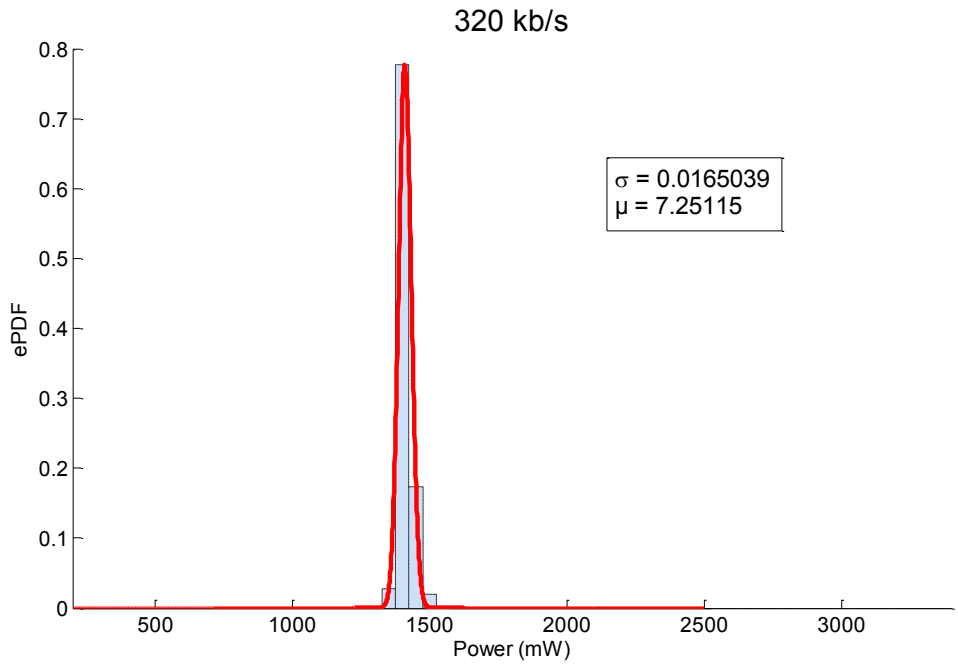

Figure C.13: Log-normal distribution of downlink in UMTS at 320 kb/s with 90% of quality signal.

Energy consumed measured: 169.2432 J.
Energy consumed modeled: 169.2435 J.

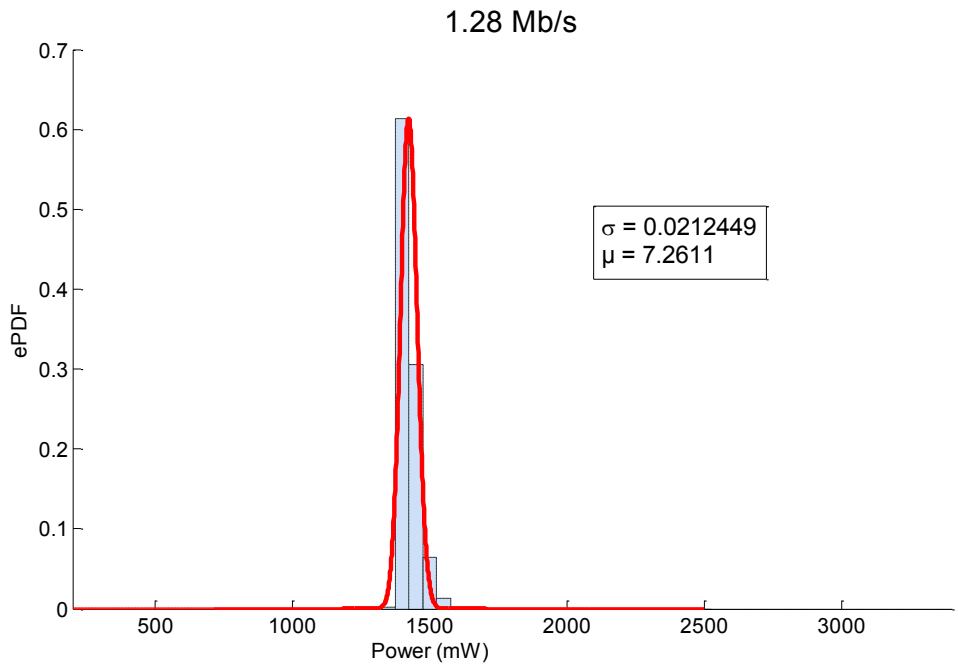

Figure C.14: Log-normal distribution of downlink in UMTS at 1.28 Mb/s with 90% of quality signal.

Energy consumed measured: 171.5652 J.
Energy consumed modeled: 171.5636 J.

LTE.

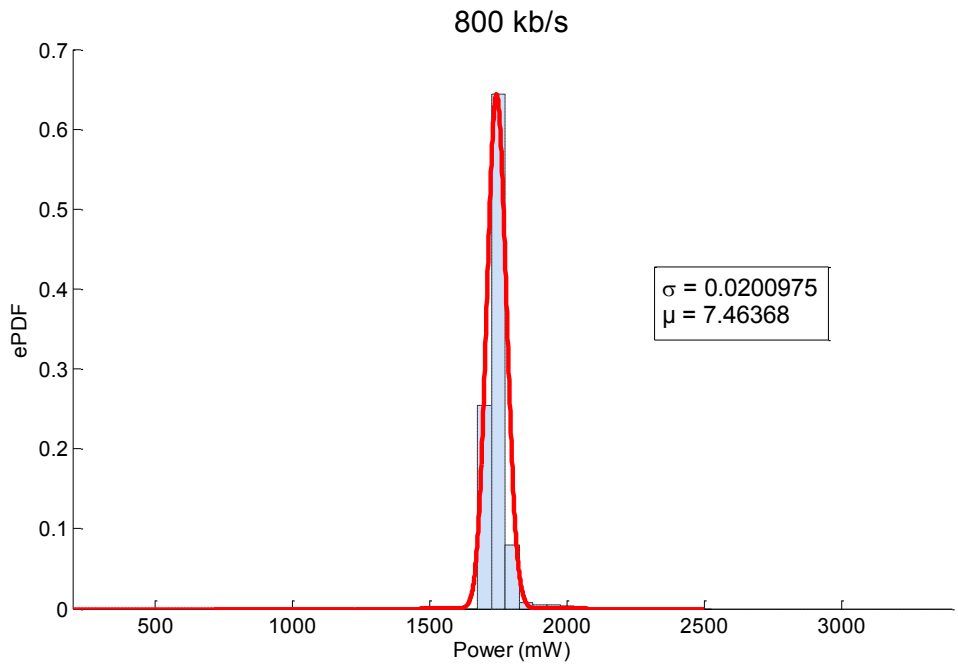

Figure C.15: Log-normal distribution of downlink in LTE at 800 kb/s with 90% of quality signal.

Energy consumed measured: 209.4048 J.
Energy consumed modeled: 209.4045 J.

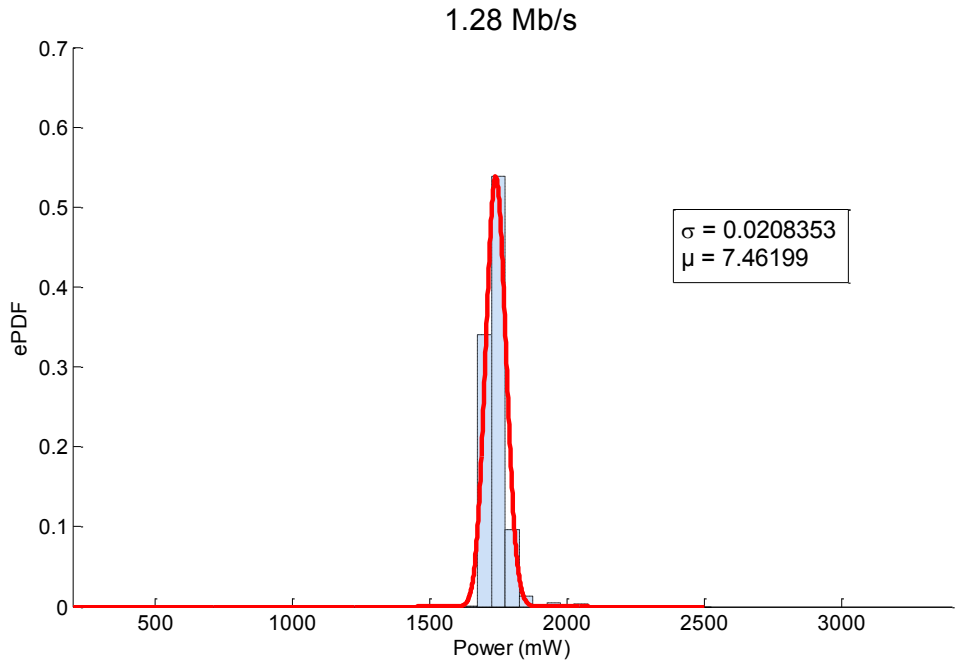

Figure C.16: Log-normal distribution of downlink in LTE at 1.28 Mb/s with 90% of quality signal.

Energy consumed measured: 210.1824 J.
Energy consumed modeled: 210.1827J.

Bibliography.

[1] J.M. Hernando, Comunicaciones Móviles, Ramón Areces S.A., Second Edition 2004.

[2] T.S. Rappaport, Wireless Communications: principles and practice, Prentice-Hall, IEEE Pres, 1996.

[3] Comunicaciones móviles digitales. Rafael Herradón. EUITT, 2005.

[4] Ericsson Mobility Report 2013.

[5] Junxian Huang, Feng Qian, Alexandre Gerber, Z. Morley Mao, Subhabrata Sen, Oliver Spatscheck. A close examination of performance and power characteristics of 4g LTE networks. University of Michigan. AT&T Labs-Research.

[6] J.M. Hernando y C. Lluch. Comunicaciones Móviles de Tercera Generación Vols I y II. Telefónica Móviles España S.A., 2000.

[7] Cisco Visual Networking Index: Global Mobile Data Traffic Forecast Update, 2013–2018.

[8] N. Balasubramanian, A. Balasubramanian, and A. Venkataramani. Energy consumption in mobile phones: A measurement study and implications for network applications. In Internet Measurement Conference, 2009.

[9] H. Falaki, D. Lymberopoulos, R. Mahajan, S. Kandula, and D. Estrin. A First Look at Traffic on Smartphones. In Internet Measurement Conference, 2010.

[10] P. Perala, A. Barbuzzi, G. Boggia, and K. Pentikousis. Theory and Practice of RRC State Transitions in UMTS Networks. In *Proc. of IEEE Broadband Wireless Access Workshop*, 2009.

[11] C.-C. Lee, J.-H. Yeh, and J.-C. Chen. Impact of inactivity timer on energy consumption in WCDMA and CDMA2000. In IEEE Wireless Telecomm. Symp.(WTS), 2004.

[12] H. Liu, Y. Zhang, and Y. Zhou. TailTheft: Leveraging the wasted time for saving energy in cellular communications. In MobiArch, 2011.

[13] F. Qian, Z. Wang, A. Gerber, Z. M. Mao, S. Sen, and O. Spatscheck. Characterizing radio resource allocation for 3G networks. In Internet Measurement Conference, 2010.

[14] J.-H. Yeh, C.-C. Lee, and J.-C. Chen. Performance analysis of energy consumption in 3GPP networks. In IEEE Wireless Telecomm. Symp. (WTS), 2004.

[15] J.-H. Yeh, J.-C. Chen, and C.-C. Lee. Comparative Analysis of Energy-Saving Techniques in 3GPP and 3GPP2 Systems. *IEEE transactions on vehicular technology*, 58(1), 2009.

[16] H. Falaki, R. Mahajan, S. Kandula, D. Lymberopoulos, and R. G. D. Estrin. Diversity in Smartphone Usage. In *Mobisys*, 2010.

[17] H. Holma and A. Toskala. HSDPA/HSUPA for UMTS: High Speed Radio Access for Mobile Communications. John Wiley and Sons, Inc., 2006.

[18] F. Liers, C. Burkhardt, and A. Mitschele-Thiel. Static RRC Timeouts for Various Traffic Scenarios. In *PIMRC*, 2007.

[19] H. Holma and A. Toskala. WCDMA for UMTS: HSPA Evolution and LTE. John Wiley and Sons, Inc., 2007.

[20] A. Schulman, V. Navda, R. Ramjee, N. Spring, P. Deshpande, C. Grunewald, K. Jain, and V. Padmanabhan. Bartendr: A Practical Approach to Energy-aware Cellular Data Scheduling. In *Mobicom*, 2010.

[21] L. Zhang, B. Tiwana, Z. Qian, Z. Wang, R. Dick, Z. M. Mao, and L. Yang. Accurate Online Power Estimation and Automatic Battery Behavior Based Power Model Generation for Smartphones. In *CODES+ISSS*, 2010.

[22] F. Qian, Z. Wang, A. Gerber, Z. M. Mao, S. Sen, and O. Spatscheck. TOP: Tail Optimization Protocol For Cellular Radio Resource Allocation. In ICNP, 2010.

[23] J. Huang, F. Qian, A. Gerber, Z. M. Mao, S. Sen, and O. Spatscheck. A close examination of performance and power characteristics of 4G LTE networks. In MobiSys, 2012.

List of Figures.